

AUTHOR'S RESPONSES TO EXECUTIVE EDITOR

In my role as Executive editor of GMD, I would like to bring to your attention our Editorial:
http://www.geoscientific-model-development.net/gmd_journal_white_paper.pdf

<http://www.geosci-model-dev.net/6/1233/2013/gmd-6-1233-2013.html>

This highlights some requirements of papers published in GMD, which is also available on the GMD website in the 'Manuscript Types' section:

http://www.geoscientific-model-development.net/submission/manuscript_types.html

Comment from Editor:

In particular it would be helpful to the reader to add the oceans model name and version to the title and maybe also the setup name. I noticed that you submitted to the NEMO special issue, but this is not instantaneously clear to a reader looking at the general list of GMD articles. Therefore I suggest to change the title to "Evaluation of an operational ocean model (NEMO2.3) configuration at 1/12_ spatial resolution for the Indonesian seas (INDO12). Part II: Biogeochemistry" in accordance to our Editorial upon revision for the final publication in GMD.

Author's response:

As suggested, we changed the title. Now, it is:

"Evaluation of an operational ocean model configuration at 1/12° spatial resolution for the Indonesian seas (NEMO2.3/INDO12). Part II: Biogeochemistry"

Comment from Editor:

Additionally I would like to encourage you to add a Code and Data Availability section at the end of the article stating how NEMO and your specific setup can be accessed by other scientists.

Author's response:

We add a new section '**Code and Data Availability**' at the end of the manuscript:

"The INDO12 configuration is based on the NEMO 2.3 version developed by the NEMO consortium. All specificities included in the NEMO code version 2.3 are now freely available in the recent version NEMO 3.6 (<http://www.nemo-ocean.eu>). The biogeochemical model PISCES is coupled to hydrodynamic model by the TOP component of the NEMO system. PISCES 3.2 and its external forcing are also available via the NEMO web site. World Ocean Database and World ocean Atlas are available at <https://www.nodc.noaa.gov>. Glodap data are available at <http://cdiac.ornl.gov/oceans/glodap/GlopDV.html>. MODIS and MERIS ocean colour products are respectively available at <http://oceancolor.gsfc.nasa.gov/cms/> and <http://hermes.acri.fr/>, Primary production estimates based on VGPM, Eppley and CbPM algorithms at <http://www.science.oregonstate.edu/ocean.productivity/>."

AUTHOR'S RESPONSES TO REFEREE 1

The manuscript 'Evaluation of an operational ocean model configuration at 1/12_ spatial resolution for the Indonesian seas – Part 2: Biogeochemistry' by Gutknecht et al. presents the marine biogeochemistry component of a high-resolution operational ocean model over the Indonesian seas. The authors conduct a thorough skill assessment of simulated biogeochemical fields from nutrients to the mesozooplankton against available satellite-derived product, climatologies and field measurements. The manuscript is overall well-written and demonstrates the good accuracy of this model configuration to replicate regional distribution of observed biogeochemical tracers. Nevertheless, I think this paper could be structured more efficiently and needs some clarification that have to be addressed first, and which prevent me of accepting this paper in its present form. Therefore, I recommend acceptance of this manuscript after some minor revisions.

We thank the reviewer for his thorough evaluation and constructive comments. We considered his suggestions carefully and provide a point-by-point reply below.

Major comments:

(1) While I acknowledge that several dataset employed in this study precludes to investigate interannual variability of some biogeochemical tracers, some of them can be used still (e.g., satellite-derived observations). Regarding the target of this operational configuration (up to monitor fisheries), assessing the interannual variability of the low trophic levels seems to be relevant.

Author's response:

We agree with the reviewer that a skillful representation of interannual variability of first trophic levels is of great relevance for this operational configuration. We added a description of climate modes in Section 2 Area of Study, and an assessment of interannual anomalies of chlorophyll-a for the period 2008-2014 in Section 5.3. The analysis points to the importance of modes of natural variability (e.g. ENSO, IOD) as drivers for interannual variability. The period (6 years) is, however, too short for a rigorous assessment of the role of these drivers.

In Section 2, we added:

"In addition to the seasonal variability driven by the Asia-Australia monsoon system, other forcing such as tides, the Madden-Julian Oscillation, Kelvin and Rossby waves affect the Indonesian seas and influence the marine ecosystems (Madden and Julian, 1994; Field and Gordon, 1996; Sprintall et al., 2000; Susanto et al., 2000, 2006). Indonesian seas are also greatly influenced by climate phenomena due to its position along the equator between Asia and Australia and between the Pacific and Indian oceans. Strength and timing of the seasonal monsoon are then affected by interannual phenomena that disturb atmospheric forcings and ocean currents. Indeed, a significant correlation between the Indonesian ThroughFlow (ITF) variability and the El Niño-Southern Oscillation (ENSO) phenomena in the western Pacific Ocean is assumed (e.g. Meyers, 1996; Murtugudde et al., 1998; Potemra et al., 1997), ENSO modulating rainfall and chlorophyll-a on inter-annual timescales (Susanto et al., 2001, 2006; Susanto and Marra, 2005). ENSO can be monitored using a Multivariate ENSO Index (MEI;

Wolter and Timlin, 1993, 1998; <http://www.esrl.noaa.gov/psd/enso/mei/>). Negative values of the MEI represent the cold ENSO phase (La Niña), while positive MEI values represent the warm ENSO phase (El Niño). In the eastern Indian Ocean, large anomalies off Sumatra and Java coasts can also be explained by the Indian Ocean Dipole (IOD) Mode monitored via the Dipole Mode Index (DMI; Saji et al., 1999). A strong positive index points to abnormally strong coastal upwelling and a large phytoplankton bloom near the Java Island (Meyers, 1996; Murtugudde et al., 1999). Sea level off Java-Sumatra modulates the ITF magnitude across the archipelago. Inside the archipelago, individual effect of each climate mode is often difficult to analyse as both events influence the ITF transport. Masumoto (2002) modelling study and Sprintall and Révelard (2014) using remotely sensed altimeter data, point out the significant impact of the Indian Ocean dynamics on the ITF transport variability across the Indonesian archipelago, likely to win out over Pacific Ocean dynamics.”

A new section (Section 5.3 Interannual variability) was added to the revised manuscript:

“Figures 7, 8 and 9 present interannual anomalies of surface chlorophyll-a concentrations between 2008 and 2014 for model output and MODIS ocean colour averaged over three regions: South China Sea, Banda Sea and Sunda area. Simulated fields and satellite derived chlorophyll-a are in good agreement in terms of amplitude and phasing, with temporal correlation coefficients of 0.56 for South China Sea and Banda sea and 0.87 for Sunda area. The model simulates a realistic temporal variability suggesting that processes regulating the seasonal as well as interannual variability of the Indonesian region are correctly reproduced. While the mean seasonal cycle of chlorophyll-a is driven by the strength and timing of the seasonal Asian monsoon, anomalies are driven by interannual climate modes, such as El Niño Southern Oscillation (ENSO) and Indian Ocean Dipole (IOD).

IOD drives the chlorophyll-a interannual variability in the eastern tropical Indian ocean, with a correlation coefficient of 0.74 (Fig. 9). IOD index and anomalies of chlorophyll-a from satellite give a similar correlation coefficient of 0.7. A positive phase of IOD indicates negative SST anomaly in the south-eastern tropical Indian Ocean associated with zonal wind anomaly along the equator (Meyers, 1996). The abnormally strong coastal upwelling near the Java Island stimulates a larger phytoplankton bloom than usual (Murtugudde et al., 1999). On Banda Sea, no straightforward impact of ENSO or IOD reaches the first level of the food chain (Fig. 8). Inside the archipelago, both climate modes affect the ITF transport variability, and it is not trivial to separate the individual effect of each climate mode (Masumoto, 2002; Sprintall and Révelard, 2014). Same comment can be done for the South China sea (Fig. 7).

ENSO and IOD climate modes play a key role in the Indonesian region, but their impact on the marine ecosystem remain a complex study. The period of simulation is too short for a rigorous assessment of the role of these drivers. Direct relationship is evident only in the Indian part. But interannual anomalies of simulated chlorophyll-a compare well with satellite observations. This realistic variability suggests that interannual meteorological and ocean physical processes are captured by the model.”

(2) It is unclear to me how the authors can evaluate the water masses transformation without showing any formation-transformation diagnostics. This is maybe a direct outcomes of the companion paper. If not, I recommend to use the terms 'water mass hydrodynamics characteristics' or equivalent which are presently shown and evaluated.

Author's response:

Yes, diagnostics concerning water mass transformation are presented on the companion paper. We now clarify this point in the revised manuscript by adding a summary of the companion paper in the Introduction:

"The regional configuration of the ocean dynamics is fully described in Tranchant et al. (this volume, hereafter Part I). The physical model reproduces main processes occurring in this complex oceanic region. Ocean circulation and water mass transformation through the Indonesian Archipelago are close to observations. Eddy Kinetic Energy displays similar patterns to satellite estimates, tides being a dominant forcing in the area. The volume transport of the Indonesian ThroughFlow is comparable to INSTANT data. TS diagrams highlight the erosion of South and North Pacific subtropical waters while crossing the archipelago."

(3) The authors point the influence of external inputs but they do not assess how accurate are the product employed to force PISCES. While I acknowledge that river inputs are difficult to assess, atmospheric inputs might be evaluate against air-borne measurements or available model outputs.

Author's response:

All external inputs used to force PISCES are extensively described and discussed in the supplementary material of Aumont and Bopp (2006). In our paper, we emphasize the major role of river discharges in this region governed by the seasonal monsoon system. Rivers supply large quantities of nutrients to the ocean. We acknowledge the lack of data at the temporal and spatial resolution required to improve model forcing at the regional scale. In the conclusion section, we recommend the contracting organization of the INDO12BIO operational configuration to consider the importance of river discharge data in order to simulate realistic biogeochemical features along the coasts.

The revised manuscript (Section 3.3) was modified as follows:

"Three different sources are supplying nutrients to the ocean: atmospheric dust deposition, sediment mobilization, and rivers. Atmospheric deposition of iron comes from the climatological monthly dust deposition simulated by the model of Tegen and Fung (1995), and Si following Moore et al. (2002). Yearly river discharges are taken from the Global Erosion Model (GEM) of Ludwig et al. (1996) for DIC, and from Global News 2 climatology (Mayorga et al., 2010) for nutrients. A constant iron source from sediment reductive mobilization on continental margins is also considered. For more details on external supply of nutrients, please refer to the supplementary material of Aumont and Bopp (2006)."

Specific comments:

P 6670 L1 'D'velopment

Author's response: Sorry, we corrected this typing error.

L10 coupled and 'on-line' are redonant.

Author's response: We feel that it is important to specify the mode of coupling, in this case "on-line", as PISCES can also be coupled to OPA/NEMO in a "off-line" mode. We are sorry if these words appear to be redundant.

L10 degradation is mentioned several times in the ms. I recommend the authors to explain a bit these terms if they are useful for the study or to remove them if they do not.

Author's response: Yes, you are right. On the revised manuscript we removed the term "degradation" as it is not usefull for the study.

L14 please reword this sentence because the papers focuses on the last 4 years of the simulation.

Author's response: As we now include interannual analysis in the revised version of the paper, we investigate the all years of the simulation expect the first one.

As a result, we modified the text in the abstract but also in Section 3.4:

- in the abstract: "The reference hindcast simulation covering the last 8 years (2007-2014) is evaluated against satellite, climatological and in-situ observations."

- in Section 3.4: "For comparison with satellite products (chlorophyll-a, primary production), we presents annual mean for year 2011 as an example. For comparison with climatologies (zooplankton, nutrients, oxygen) and analysis of the seasonal cycle, we are using years 2010 to 2014. For interannual variability, we consider the whole length of simulation except the first year, so 2008 to 2014."

L25 'water mass hydrodynamics and biogeochemical properties' ?

L26 vertical distribution of what ?

Author's response: We reformulate the this sentence in the abstract to:

"Vertical distribution of nutrient and oxygen is comparable to in-situ based datasets although slightly smoothed. Biogeochemical characteristics of North Pacific tropical waters entering in the archipelago are realistic. Hydrodynamics transformation of water masses across the Indonesian archipelago allows conserving nitrate and oxygen vertical distribution close to observations, in Banda Sea and at the exit of the archipelago."

P6671

L25 change 'but propagate' into 'but also propagate'

Author's response: We changed 'but propagate' into 'but also propagate'

P6672

L7 Change 'capacity' into 'capability'

Author's response: We changed 'capacity' into 'capability'

L9 Madec et al. 2008 shall be preferred regarding the NEMO model version

Author's response: Yes, you are right, we changed the reference.

P6674

L26 please confirms that NEMO3.2 is used.

Author's response: OPA/NEMO version 2.3 is used

P6675

L17 Do you refer to the standard PISCES set of parameters?

Author's response: We used the standard PISCES set of parameters in its version 3.2, except for 2 parameters. Indeed, a sensitivity analysis focused on the half-saturation constant for phytoplankton growth. We tested each half-saturation constant of the model by dividing or multiplying the constant by a factor 2 as compared to the standard 3.2 namelist. We focussed on nanophytoplankton species as we aimed to decrease the chlorophyll-a concentrations in the open ocean. After all, an increase by a factor two of the half-saturation constant for NO_3 , NH_4 and PO_4 assimilation (conc0 and concnnh4 parameters in the namelist) leads to slightly lower surface chlorophyll-a concentrations in the open ocean after some months of simulation. But after several years and monthly or annually averages, the impact is negligible, especially compared to the change of advection scheme (MUSCL vs QUICKEST-Zalezak). As discussed in the Discussions and Conclusions Section, the change in advection scheme impacts the biogeochemical tracer distribution to the first order. Ideally, we should have re-run the simulation with the standard PISCES namelist, but due to computing cost, this was not possible. It was decided to keep the 2 modifications. However, we chose not to detail this sensitivity study in the submitted paper due to its lack of significance.

P6676

L6 please expand the TOP acronym and explain its function. Is this another module coupled to PISCES ?

Author's response: TOP is the component that allows the biogeochemical model PISCES to be coupled with NEMO-OPA ocean dynamics model. NEMO-TOP resolves the advection/diffusion equations of passive tracers as well as biogeochemical sources minus sinks if a biogeochemical model is activated, here PISCES.

We added a sentence in Section 3 to clarify what is TOP component:

“PISCES is coupled to NEMO-OPA via the TOP component that manages the advection/diffusion equations of passive tracers but also the sources and sinks terms due to biogeochemistry.”

I think that merging the PISCES description with the 3.1 section could make the model setup clearer.

Author's response: For the revised version, we merged the NEMO and PISCES description with the Section 3.1 “The coupled model” to make the model setup clearer.

Few words on the Redfieldian assumption of PISCES provided in the ms can be also detailed here.

Author's response:

Redfieldian assumption of PISCES has been clarified in Section 3.1 of the revised version.

“Constant C/N/P Redfield ratios are supposed for all species. While internal Fe/C and Si/C ratios of phytoplankton are modelled as a function of the external availability of nutrients and thus variable, only C is prognostically modelled for zooplankton.”

Please check the references of external inputs? (It seems to me that atmospheric dust deposition were derived from Tegen and Fung, (1995))

Author's response:

You are right, we corrected the references of external inputs; atmospheric dust deposition comes from the model of Tegen and Fung (1995).

P6677

Section 4: I suggest to re-order subsection with (1) INDOXMIX measurements which presents hydrodynamics properties, (2) nutrients and finally (3) ecosystems parameters.

Author's response: We reordered Section 4 as suggested.

L14 please indicate the exact period of the simulation

Author's response: We now clarify the exact period of the simulation in Section 3.4:

“The simulation started on January 3rd, 2007 and operates up to present day as the model currently delivers ocean forecasts. But for the present paper, we will analyse the simulation up to December 31, 2014.”

L20 please provide the evolution of tracers' concentrations at various depth because 3D average generally masks drift. Please give few metrics to quantify the steady state of the tracers' concentrations.

Author's response:

The objective of Figure 1 is to demonstrate the model has a satisfying behaviour all along the simulation length, without drift due to mass conservation problems. To this end, tracers' concentrations over the whole 3D domain are presented. Strictly speaking, the model can not reach steady state as open boundary conditions and surface forcing come from global forecasting systems. Interannual variability, as well as temporal drift is introduced in the domain configuration.

We follow, however, the suggestion put forward by the reviewer and add the following figures to the supplementary material.

Figures A to F present the evolution of tracers' concentrations at various depths: surface, 0-100m, 100-600m and 600m-bottom, in order to detect abnormal drift with time. Please find as example the evolution of nutrients, chlorophyll-a and net primary production (NPP), but also the main stressors of marine ecosystems: sea surface temperature (SST) and oxygen concentrations. It can be seen that:

(1) Chlorophyll-a and NPP do not significantly drift over the time of the simulation (Figure A), with an averaged chlorophyll-a concentration about $0.51 \text{ mg Chl m}^{-3}$ at the surface and $0.35 \text{ mg Chl m}^{-3}$ between 0-100m and vertically integrated NPP about $58.9 \text{ mmol C m}^{-2} \text{ d}^{-1}$.

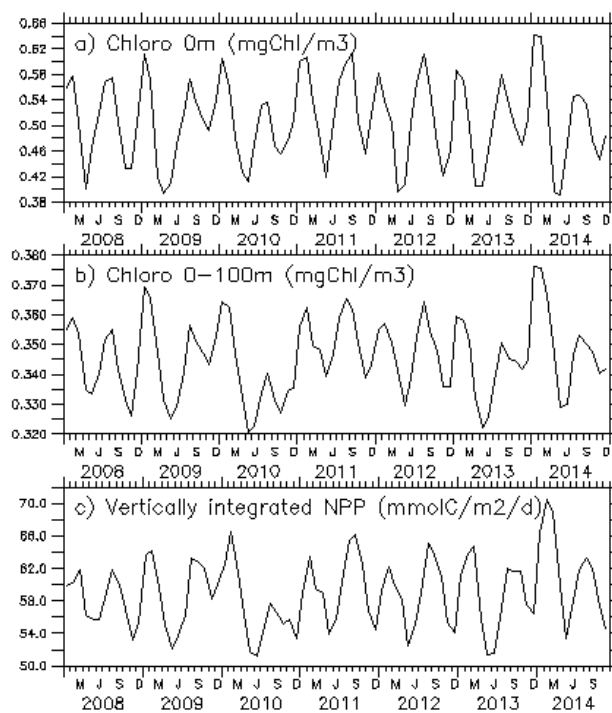


Figure A: Temporal evolution of chlorophyll-a concentrations at the surface (a) and in the first 100m depths (b) and vertically integrated NPP (c), averaged over the whole INDO12BIO domain.

(2) Nutrients do not present a clear trend, but display a vertical adjustment in course of simulation (Figures B, C, D and E; please note different scales on ordinate axes). Nitrogen and Phosphate are

almost stable in the upper 100m. They slightly decrease at depth (600-to bottom) during the first years of simulation and then increase the following years. Dissolved Si increases in the top 600m and decreases below. Conversely, dissolved Fe decreases in the 100 to 600m depth interval and increases below.

(3) Dissolved oxygen does not present a clear trend in the first 100m (Figures B and C). However, over the whole 3D domain, a mean drift of $-0.006 \text{ ml O}_2 \text{ l}^{-1} \text{ yr}^{-1}$ is simulated by the model. The strongest negative trends are mainly located in the top 200m, in the archipelago (South China Sea, Banda Sea, and semi-enclosed areas), but also in the open ocean (not shown). Some areas also exhibit positive trends. The strongest are found in the Pacific and Indian parts of the model domain and are mainly situated between 300 and 1500m depth (not shown). Again a negative oxygen trend is simulated below. As for nutrients, the model reorganizes the vertical distribution of oxygen during the simulation.

(4) The simulated time series of SST (Figure F) is compared to the Reynolds product based on remotely sensed SST data. The positive bias is discussed in Tranchant et al. (this volume). Here, we are more interested by the phasing and the temporal trend between simulated and observed SST. Temporal variations are realistically simulated by the model, with an excellent correlation between the two time series ($r = 0.94$). Simulated monthly averaged SST presents a positive trend of $+0.023^\circ\text{C yr}^{-1}$. Monthly averaged Reynolds SST indicates a positive trend of $+0.032^\circ\text{C yr}^{-1}$.

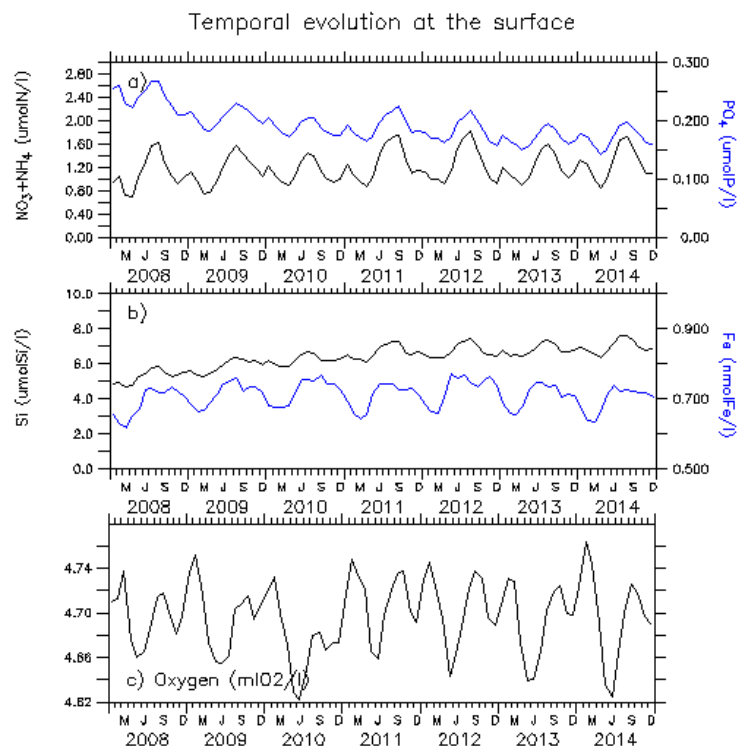


Figure B: Temporal evolution of nutrient (nitrate+ammonium, phosphate, Dissolved Si, and Dissolved Fe) and oxygen content at the surface, averaged over the whole INDO12BIO domain.

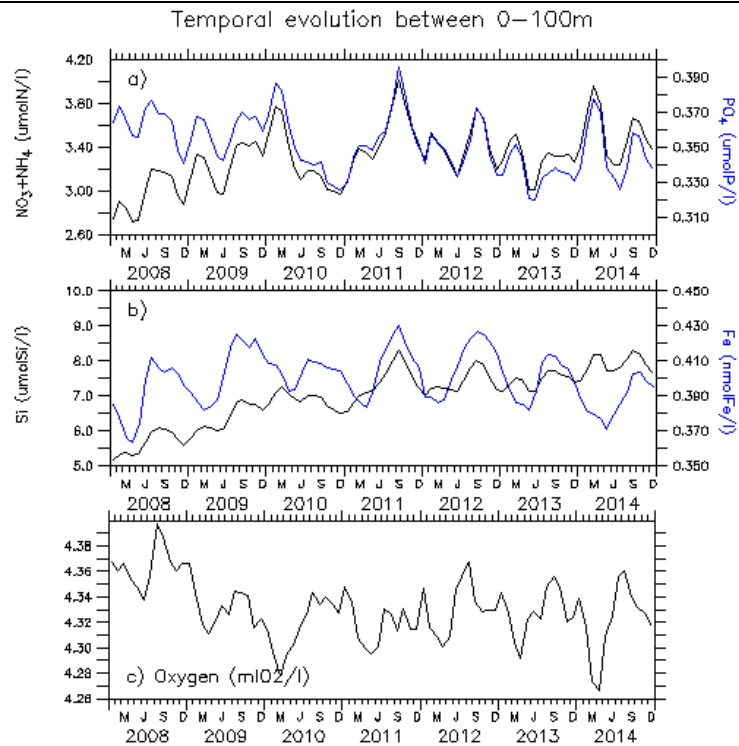


Figure C: Temporal evolution of nutrient (nitrate+ammonium, phosphate, Dissolved Si, and Dissolved Fe) and oxygen content in the first 100m depths, averaged over the whole INDO12BIO domain.

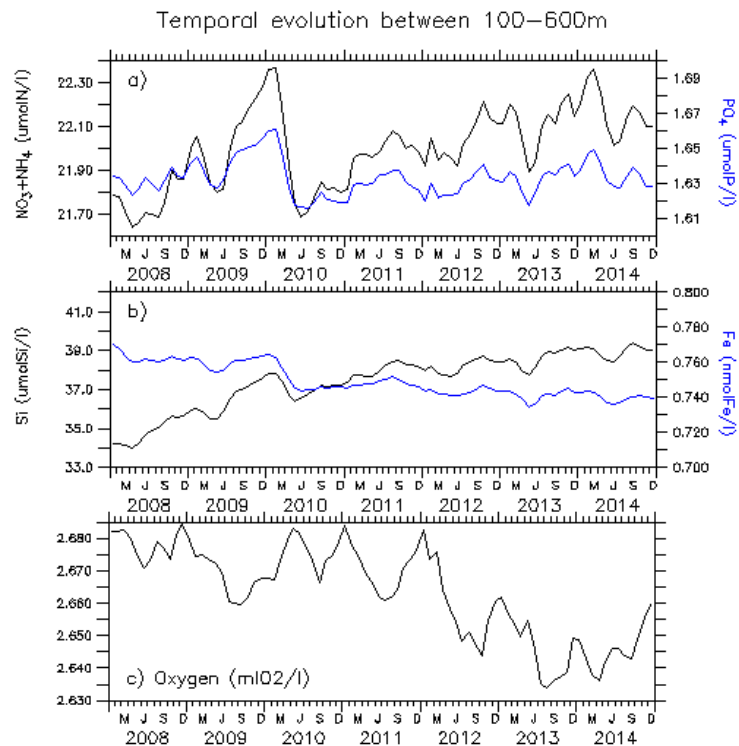


Figure D: Temporal evolution of nutrient (nitrate+ammonium, phosphate, Dissolved Si, and Dissolved Fe) and oxygen content between 100 and 600m depths, averaged over the whole INDO12BIO domain.

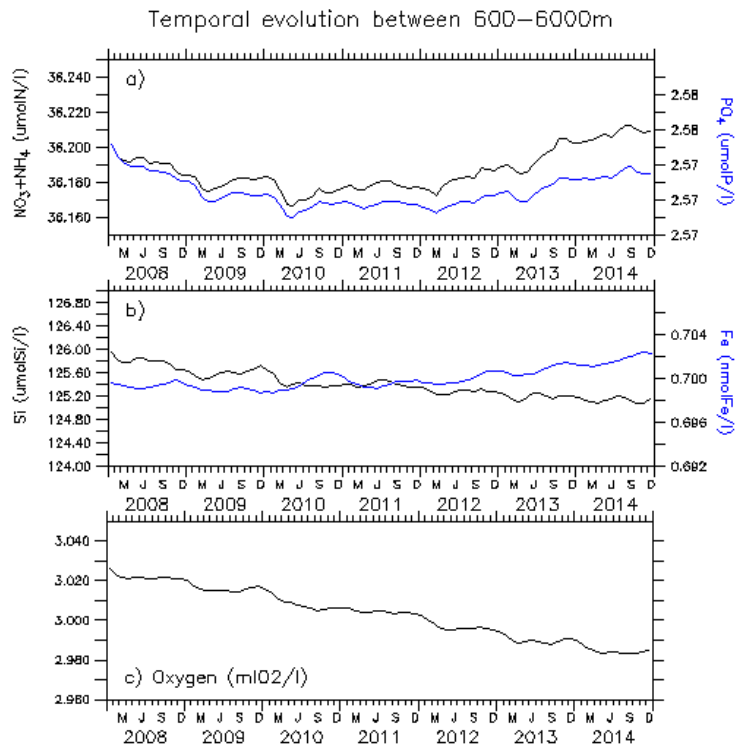


Figure E: Temporal evolution of nutrient (nitrate+ammonium, phosphate, Dissolved Si, and Dissolved Fe) and oxygen content at depth (between 600 and 6000m depths), averaged over the whole INDO12BIO domain.

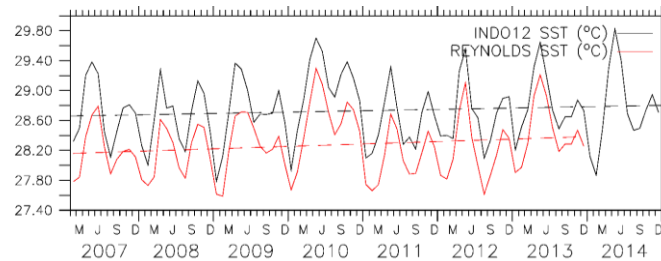


Figure F: Temporal evolution of Sea Surface Temperature over the whole domain (solid line) and associated trend (dashed line), computed from INDO12BIO monthly outputs (black) and from Reynolds satellite product (red).

To conclude, the model tends towards a “steady state”, in terms of numerical equilibrium. There is no loss of material (temperature, carbon, oxygen, ...) due to numerical deviation. For the physical part, a realistic temporal trend is simulated in SST as compared to satellite data. For biogeochemistry, chlorophyll-a and NPP are almost stable during the time of the simulation, while nutrients and oxygen need a longer-term vertical adjustment.

However, it is not straightforward to conclude on a potential drift of the model as the simulation is too short to estimate accurate temporal trends, and the region has very few data to compare with. This is why we did not include these plots to the main section of revised version, but decided to add them to the supplementary material. However, in the revised version, we now include the interannual variability of chlorophyll-a.

P6679

Section 4.2 : please refer to Henson et al. (2010) which used several satellite-derived algorithm to compute phytoplankton production. This paper is of interest for this study since it discuss the uncertainty of the CbPM algorithm compared to the others.

Author's response: Yes, we are aware that CbPM gives results substantially different from the other algorithms. We now clarify this point in the revised version. But we are keen to present the dispersion between satellite-based algorithms, and more particularly in this region where uncertainties concerning satellite optical measurements can be great due to river discharges and shallow water depths that disturb the signal.

We added the following sentence to the revised manuscript (Section 4.4): "Henson et al. (2010) point the uncertainty of the CbPM algorithm, giving results substantially different from the other algorithms."

L14 please give a reference for MAREDAT.

Author's response: Sorry, we added the reference to MAREDAT atlas:

Buitenhuis, E. T., Vogt, M., Moriarty, R., Bednaršek, N., Doney, S. C., Leblanc, K., Le Quéré, C., Luo, Y.-W., O'Brien, C., O'Brien, T., Peloquin, J., Schiebel, R., and Swan, C.: MAREDAT: towards a world atlas of MARine Ecosystem DATA, Earth Syst. Sci. Data, 5, 227-239, doi:10.5194/essd-5-227-2013, 2013.

P6680

L4 Please explain. In PISCES, phytoplankton growth is limited by the various nutrients concentration (e.g., Laufkötter et al., 2015). Therefore, nitrate and phosphate should be decoupled in the model.

Author's response:

Yes, growth rate of phytoplankton is limited by the external availability in N, P, Si and Fe. Stoichiometry of C/N/P is fixed in PISCES. So nitrate+ ammonium and phosphate are not independent nutrients. We clarified this point in Section 3.1.

For the Indonesian configuration, we only present nitrate, and dissolved Si distributions in the submitted paper, as phosphate gives similar results to nitrate.

Section 5: Here also, I suggest to re-order the subsection by presenting (1) annual mean state nutrients and ecosystem parameters and (2) seasonal to interannual variability of some biogeochemical fields (if Chl and NPP have reached a steady state before 2010). According to Gierach et al. (2012), the 2009-2010 ENSO event has implications on the biological fields.

Author's response: As suggested, we reordered the Section 5 in 5.1 Annual mean state; 5.2 Mean seasonal cycle; 5.3 Interannual variability; 5.4 INDOMIX cruise.

Yes ENSO event and also IOD phenomena have implications on the biological fields. It is now discussed in Section 5.3 Interannual variability.

P6686,

L17 please detail what water mass transformation means.

Author's response: We reformulated the sentence in Section 6 to:

“Biogeochemical characteristics of North Pacific tropical waters entering in the archipelago are set by the open boundary. Hydrodynamics transformation of water masses across the Indonesian archipelago are simulated satisfyingly. As a result, nitrate and oxygen vertical distributions match observations in Banda Sea and at the exit of the archipelago.”

References:

Gierach, M. M., Lee, T., Turk, D. and McPhaden, M. J.: Biological response to the 1997-98 and 2009-10 El Niño events in the equatorial Pacific Ocean, *Geophys. Res. Lett.*, 39(10), L10602, doi:10.1029/2012GL051103, 2012.

Henson, S. A., Sarmiento, J. L., Dunne, J. P., Bopp, L., Lima, I., Doney, S. C., John, J. and Beaulieu, C.: Detection of anthropogenic climate change in satellite records of ocean chlorophyll and productivity, *Biogeosciences*, 7(2), 621–640, doi:10.5194/bg-7-621-2010, 2010.

Laufkötter, C., Vogt, M., Gruber, N., Aita-Noguchi, M., Aumont, O., Bopp, L., Buitenhuis, E., Doney, S. C., Dunne, J., Hashioka, T., Hauck, J., Hirata, T., John, J., Le Quéré, C., Lima, I. D., Nakano, H., Séférian, R., Totterdell, I., Vichi, M. and Völker, C.: Drivers and uncertainties of future global marine primary production in marine ecosystem models, *Biogeosciences Discuss.*, 12(4), 3731–3824, 2015.

Tegen, I. and Fung, I.: Contribution to the Atmospheric Mineral Aerosol Load From Land-Surface Modification, *J Geophys Res-Atmos*, 100, 18707–18726, 1995.

AUTHOR'S RESPONSES TO REFEREE 2

We thank the reviewer for his careful reading of our manuscript. We considered his suggestions and critics. A point-by-point reply is presented hereafter.

General comments:

1. important details about the model simulation are lacking
- do you include tidal mixing?

Author's response 1:

We acknowledge the importance of tidal mixing.

A parameterization of the vertical mixing induced by internal tides has especially been developed for OPA/NEMO, by artificially enhancing vertical viscosity and diffusion coefficients, and gives satisfying results on Indonesian seas (Koch-Larrouy et al., 2007, 2010). While it considered in this study, it is part of the physical configuration. All technical aspects concerning the physical configuration are detailed in the companion paper (Tranchant et al., submitted).

We nevertheless added a sentence to Section 3.1 of the revised paper: "A parameterization of the vertical mixing induced by internal tides has especially been developed for OPA/NEMO (Koch-Larrouy et al., 2007, 2010).".

- you fixed mean run off and nutrient supply. Is this realistic for such a dynamic environment.

Author's response 2:

We thank the reviewer for highlighting the importance of river nutrient supply.

For physical runoff, a monthly global climatology is built with data on coastal runoffs and 99 major rivers from Dai and Trenberth (2002) and prescribed with a flux formulation into the model. In addition, two important missing rivers (Mahakam and Kapuas on Borneo Island) with large enough rates (class 3) were added to this database.

For nutrient supply, we are forced to use an annual climatology for want of observations at high temporal resolution. In the paper, we point to the major role of river discharges in this region governed by the seasonal monsoon system, which supply huge quantity of nutrients to the ocean. We also concede that at present data are lacking to improve model forcing by river nutrient input. Figure 11 of the revised manuscript presents the poor temporal correlation between the modelled chlorophyll-a and satellite data along the coasts. On the conclusion part, we recommend the contracting organization of this operational configuration to consider the importance of river discharges in order to simulate realistic biogeochemical features along the coasts.

- it is a short simulation and I would like to see some upper ocean diagnostics to show how key fields like NPP and surface phytoplankton, nitrate, iron and silicate evolve over the simulation. Do the model upper ocean nutrients drift with time?

- should show for the domain what the difference in the nutrient fields between the start and end of the simulation as a depth time plot of the annual change in nutrients over the simulated period reference to the start of the simulation.

Author's response 3:

The objective of Figure 1 is to demonstrate the model has a satisfying behaviour all along the simulation length, without drift due to mass conservation problems. To this end, tracers' concentrations over the whole 3D domain are presented. Strictly speaking, the model can not reach steady state as open boundary conditions and surface forcing come from global forecasting systems. Interannual variability, as well as temporal drift is introduced in the domain configuration.

We follow, however, the suggestion put forward by the reviewer and add the following figures to the supplementary material. Figures A to F present the evolution of tracers' concentrations at various depths: surface, 0-100m, 100-600m and 600m-bottom, in order to detect abnormal drift with time. Please find as example the evolution of nutrients, chlorophyll-a and net primary production (NPP), but also the main stressors of marine ecosystems: sea surface temperature (SST) and oxygen concentrations. It can be seen that:

(1) Chlorophyll-a and NPP do not significantly drift over the time of the simulation (Figure A), with an averaged chlorophyll-a concentration about 0.51 mg Chl m⁻³ at the surface and 0.35 mg Chl m⁻³ between 0-100m and vertically integrated NPP about 58.9 mmol C m⁻² d⁻¹.

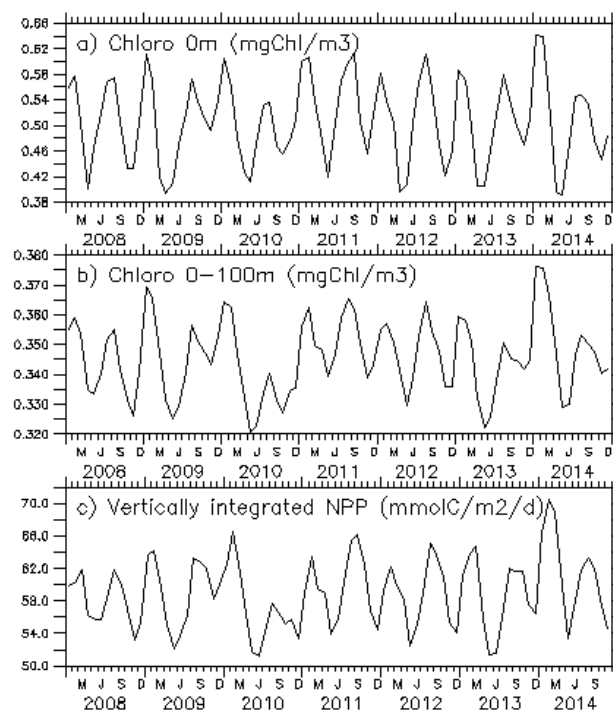


Figure A: Temporal evolution of chlorophyll-a concentrations at the surface (a) and in the first 100m depths (b) and vertically integrated NPP (c), averaged over the whole INDO12BIO domain.

(2) Nutrients do not present a clear trend, but display a vertical adjustment in course of simulation (Figures B, C, D and E; please note different scales on ordinate axes). Nitrogen and Phosphate are almost stable in the upper 100m. They slightly decrease at depth (600-to bottom) during the first years of simulation and then increase the following years. Dissolved Si increases in the top 600m and decreases below. Conversely, dissolved Fe decreases in the 100 to 600m depth interval and increases below.

(3) Dissolved oxygen does not present a clear trend in the first 100m (Figures B and C). However, over the whole 3D domain, a mean drift of $-0.006 \text{ ml O}_2 \text{ l}^{-1} \text{ yr}^{-1}$ is simulated by the model. The strongest negative trends are mainly located in the top 200m, in the archipelago (South China Sea, Banda Sea, and semi-enclosed areas), but also in the open ocean (not shown). Some areas also exhibit positive trends. The strongest are found in the Pacific and Indian parts of the model domain and are mainly situated between 300 and 1500m depth (not shown). Again a negative oxygen trend is simulated below. As for nutrients, the model reorganizes the vertical distribution of oxygen during the simulation.

(4) The simulated time series of SST (Figure F) is compared to the Reynolds product based on remotely sensed SST data. The positive bias is discussed in Tranchant et al. (this volume). Here, we are more interested by the phasing and the temporal trend between simulated and observed SST. Temporal variations are realistically simulated by the model, with an excellent correlation between the two time series ($r = 0.94$). Simulated monthly averaged SST presents a positive trend of $+0.023^\circ\text{C yr}^{-1}$. Monthly averaged Reynolds SST indicates a positive trend of $+0.032^\circ\text{C yr}^{-1}$.

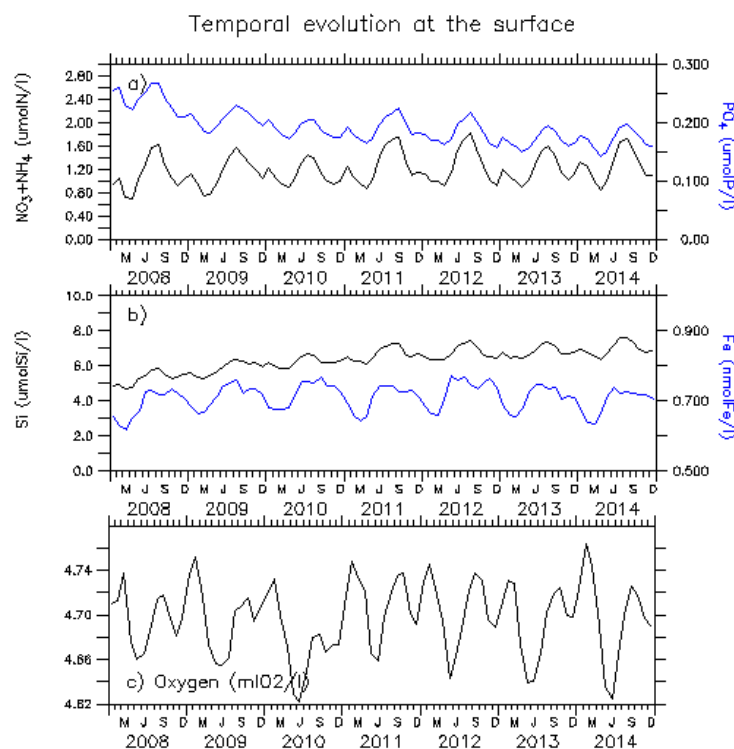


Figure B: Temporal evolution of nutrient (nitrate+ammonium, phosphate, Dissolved Si, and Dissolved Fe) and oxygen content at the surface, averaged over the whole INDO12BIO domain.

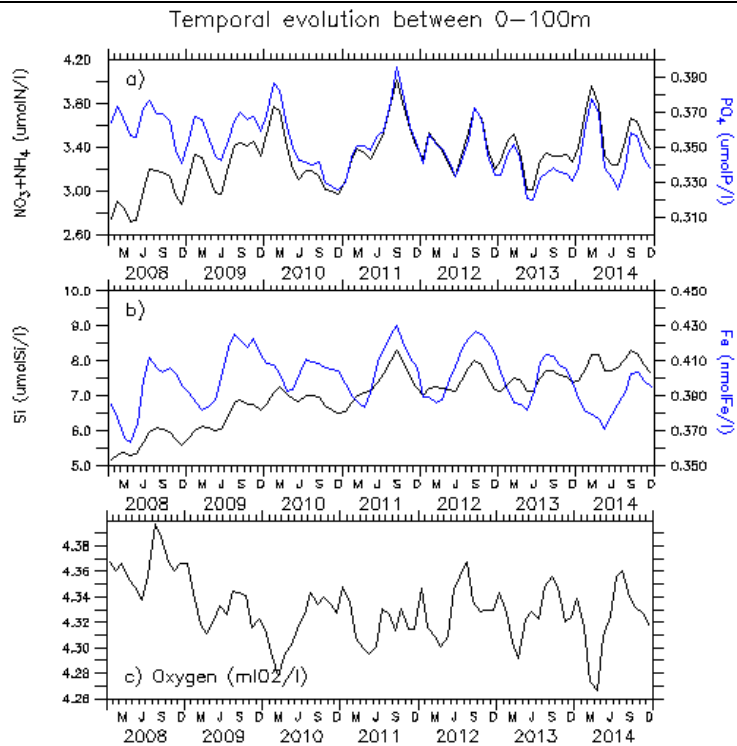


Figure C: Temporal evolution of nutrient (nitrate+ammonium, phosphate, Dissolved Si, and Dissolved Fe) and oxygen content in the first 100m depths, averaged over the whole INDO12BIO domain.

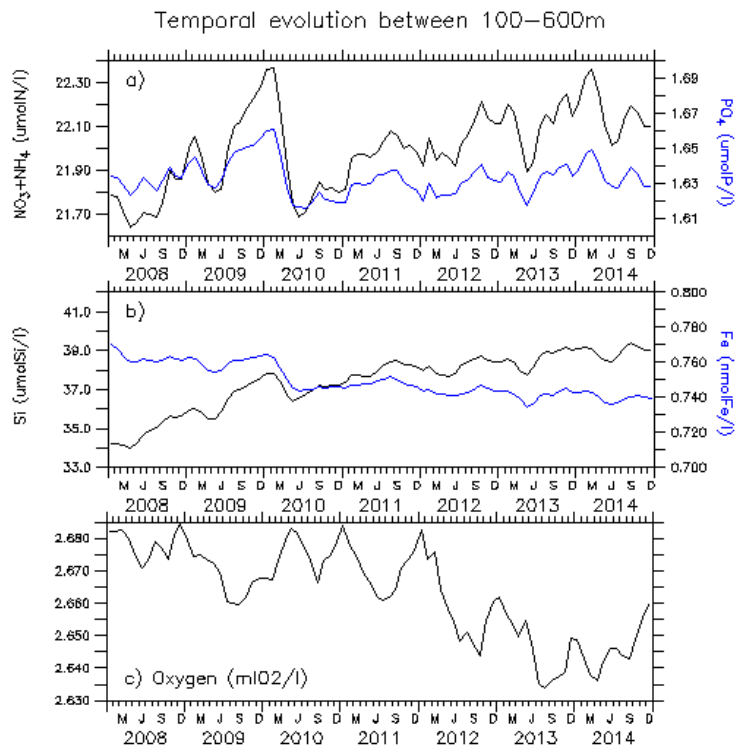


Figure D: Temporal evolution of nutrient (nitrate+ammonium, phosphate, Dissolved Si, and Dissolved Fe) and oxygen content between 100 and 600m depths, averaged over the whole INDO12BIO domain.

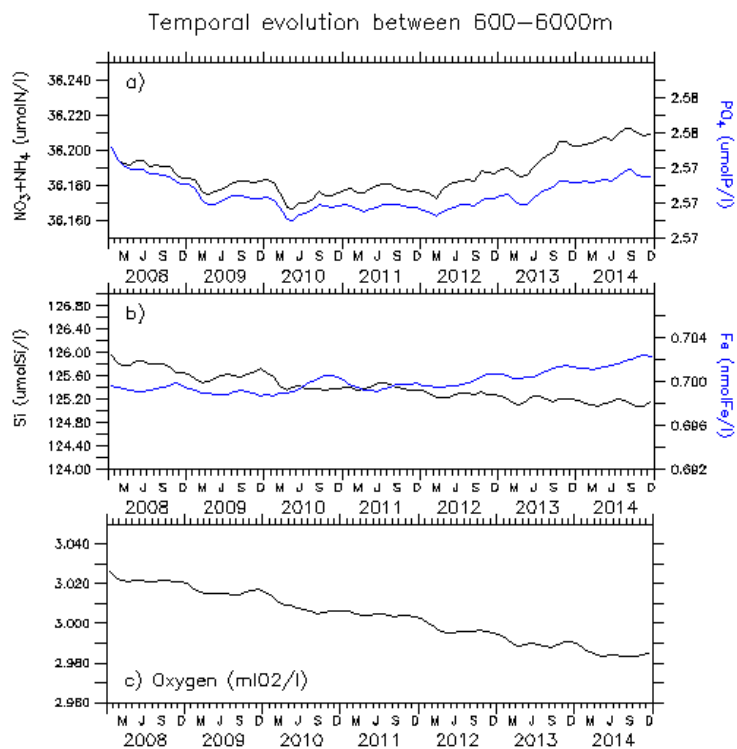


Figure E: Temporal evolution of nutrient (nitrate+ammonium, phosphate, Dissolved Si, and Dissolved Fe) and oxygen content at depth (between 600 and 6000m depths), averaged over the whole INDO12BIO domain.

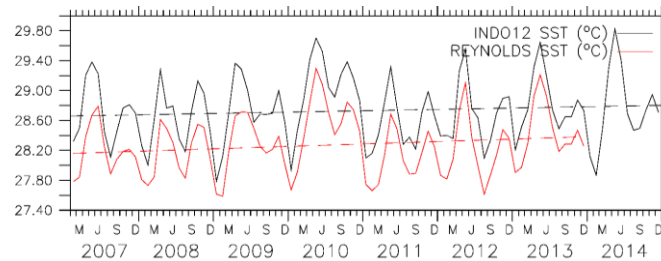


Figure F: Temporal evolution of Sea Surface Temperature over the whole domain (solid line) and associated trend (dashed line), computed from INDO12BIO monthly outputs (black) and from Reynolds satellite product (red).

To conclude, the model tends towards a “steady state”, in terms of numerical equilibrium. There is no loss of material (temperature, carbon, oxygen, ...) due to numerical deviation. For the physical part, a realistic temporal trend is simulated in SST as compared to satellite data. For biogeochemistry, chlorophyll-a and NPP are almost stable during the time of the simulation, while nutrients and oxygen need a longer-term vertical adjustment.

However, it is not straightforward to conclude on a potential drift of the model as the simulation is too short to estimate accurate temporal trends, and the region has very few data to compare with. This is why we did not include these plots to the main section of revised version, but decided to add them to the supplementary material. However, in the revised version, we now include the interannual variability of chlorophyll-a.

- in the coastal environment how important is iron supply from river run off vs iron supply from sediments? similar thoughts on the nitrate budget may also be useful.

Author's response 4:

You raise a very interesting question. However, the crucial lack of in-situ measurements prevents us to provide an answer with relevance to the region of interest. We foresee, however, that in the framework of the INDESO project more in-situ data will be sampled in the future, which will enable us to answer this question.

-Some additional details about the larger scale model that helps sets some of the boundary conditions for the regional model would be helpful. How long was this model run for, what were the initial conditions, are properties in the global simulation on the boundary of the regional model changing with time? How do they compare to the observations.

Author's response 5:

For the physics (see Tranchant et al., this volume), daily open boundary conditions are given by the Mercator-Ocean Global Ocean Forecasting System at $\frac{1}{4}^\circ$ (PSY3V3R3) (Lellouche et al., 2013) started in October 2006 from a Levitus climatology. These conditions include temperature, salinity, currents and Sea Surface Height. Open boundary conditions are located on a relaxation band of 10 grid points ($\sim 1^\circ$).

For biogeochemistry, open boundary conditions are derived from climatological data bases, satellite data, analytical values, or global model (ORCA2 simulation). The global scale model configuration ORCA2 at 2° of resolution has been integrated 3000 years, until PISCES reached a quasi steady-state with a mean state and seasonal variations similar to those observed for nutrients and chlorophyll (see Aumont and Bopp, 2006). For INDO12BIO configuration, we used a monthly climatology based on this simulation. A detailed comparison between model and data is given in the auxiliary material of Aumont and Bopp (2006).

For the revised manuscript, we now clarify this point in Section 3.2:

“For tracers for which this information is missing, initial and open boundary conditions come either from a global scale simulation, or have to be estimated from satellite data, respectively build using analytical values. The global scale model configuration ORCA2 at 2° of resolution has been integrated 3000 years, until PISCES reached a quasi steady-state with a mean state and seasonal variations similar to those observed for nutrients and chlorophyll (see Aumont and Bopp, 2006). For INDO12BIO configuration, a monthly climatology was used for dissolved iron and DOC based on this simulation.”

2. Paper states it is focused on the assessment of the simulation but little quantitative numbers are provided.

-What is the total NPP in the domain (model verse observations derived products)

- Provide quantitative assessments of the annual mean spatial variability and seasonal temporal variability of chl_a (by at least providing correlation and variance comparisons).

Author's response 6:

We preferred to present mean values, standard deviation and temporal correlation for modeled and observed chlorophyll-a on maps rather than in a table. Spatial mean and standard deviation values over the INDO12BIO domain are provided for surface chlorophyll-a and vertically integrated NPP (model and observations) in 2011 relative to Figure 4 and 5 of the revised version. The temporal correlation between modelled chlorophyll-a and estimates derived from remote sensing is spatially presented. In addition, we provide the mean temporal correlation over the entire INDO12BIO domain in the revised version.

Note the multiple data products should also be compared to provide a perspective on the acceptable agreement.

Author's response 7:

We voluntarily decided not to multiple ocean color data. We acknowledge that the error associated with satellite product is large, particularly in the coastal ocean. We clarify this point in Section 4.3. Moreover, MODIS ocean color product is the only sensor covering the entire period of simulation, so it was a natural choice.

-From the timeseries of Chl it appears the model captures the variability but overestimates the mean value - good result. Problem with Carbon to Chl use in the model? or excessive Phytoplankton in the coastal regions of the model? what is it?

Author's response 8:

We agree with the reviewer that the model overestimates the chlorophyll-a content of oligotrophic waters and that the cross-shore gradient is too weak. These systematic misfits are discussed in Section 6. We point towards the main role of the numerical advection scheme. As a matter of fact, the current advection scheme for passive tracers (MUSCL) is too diffusive and smooths vertical profiles of nutrients. As a result, too much nutrients are injected in the surface layer which triggers too high levels of production and hence chlorophyll-a.

The double peak in the Chla is also interesting, do you think this is a real feature?

Author's response 9:

The double peak in the simulated chlorophyll-a is also present in the satellite product; a double peak in South China sea, a significant secondary peak in Banda sea, and sometimes a minor secondary peak in Sunda area. The model-data comparison suggests thus that it is a realistic feature.

-Showing water properties down to 1000 m is not very useful given the short run where only significant changes in the upper ocean have a chance to develop. Further the range in values between 0 and 1000m makes it difficult to see key differences in the upper ocean. It would be helpful to show some surface plots. I would like to know what is limiting phytoplankton in the coastal areas of the simulation. How does nutrient limitation in the simulation compare to the observations ?

Author's response 10:

This comment raises several points:

- "Showing water properties down to 1000 m is not very useful given the short run where only significant changes in the upper ocean have a chance to develop." We acknowledge that due short simulation time, biogeochemical properties at depth are expected to reflect initial conditions. However, and as pointed out by the reviewer under comment 3, the regional model could potentially display strong drifts at depth. The comparison between observed and modeled biogeochemical tracer profiles provides additional means for evaluating the stability of the model. In order to improve the readability of changes in the upper ocean, we adjusted the vertical scale of Figure 3 in the revised manuscript. To allow the reader to appreciate differences in vertical gradients, profiles are still presented down to 2000m.
- "It would be helpful to show some surface plots." Surface plots are presented as part of Author's response 3, please refer to Figures A, B and F.
- "How does nutrient limitation in the simulation compare to the observations." The model allows to identify limiting factors of phytoplankton production (e.g. specific nutrient, light). There are, however, to our best knowledge no in situ data on nutrient limitation available in this area. It is does impossible to compare simulation and observations.

3. There is some discussion of the limitations of the model but some change in the organisation of this section would make it more useful. Perhaps dividing the discussion into coastal and open ocean would be better. I would also like a bit more detail on the weakness and strengths of the simulation presented.

Open Ocean

Produce the large scale seasonal variability in chl_a.

Too weak a vertical nutrient gradient in the open ocean with some issues with the water properties (e.g. silicate in the Pacific part of the domain)

- numerics of the advection scheme -> need to know how tidal mixing is prescribed since this is an important source of vertical mixing in the Indo Seas

Coastal

Too much chl_a on the shelves.

- shelf to open ocean gradients - could be linked to how river run off parameterizations. How do you assess whether it is a problem with river run off, a problem with the ocean dynamics and problem with sediment BGC. Did you consider a simulation without river run off? How important is river run off to the open ocean behaviour?

Author's response 11:

We are not certain to fully understand this recommendation. Does it refer to Section 5: Evaluation or Section 6: Discussions and conclusions ? Reviewer 1 also suggested a restructuring of Section 5. We followed his suggestion and Section 5 is now structured as: 5.1 Annual mean states (nutrients, oxygen, chlorophyll-a, NPP, zooplankton); 5.2 Mean seasonal cycle; 5.3 Interannual variability; 5.4 INDOMIX cruise.

Following your comment, we clarified Section 6 as follows: 1/ strengths of the simulation, 2/ weaknesses: coastal ocean (due to sedimentary processes and river inputs); shelves and open ocean (due to implemented numerical scheme).

Tidal mixing is described in the companion paper (Tranchant et al., submitted), and is discussed in Author's response 1 above.

The problem of shelf to open ocean gradients is related to numerical scheme. The MUSCL scheme is too diffusive and smooths vertical profiles of nutrients in the open ocean. Too much nutrients are thus injected in the surface layer and trigger too high chlorophyll-a levels and NPP. This problem is clearly identified and will be treated in a future release of the INDO12BIO operational system.

We did not consider a simulation without river run off. The contribution of river run off to setting biogeochemical characteristics of open ocean waters is an open question which deserves further investigations.

Details:

pg 2 l5- no mention of large marine predators in the paper

Author's response: As stated in the introduction, the forecasting system developed within the framework of the INDES0 project, will ultimately consist of 3 numerical models coupled physics, biogeochemistry and fish population dynamics). The focus of this paper is on the presentation and evaluation of the biogeochemical component of the suite of models. The upper trophic level model, which represents population dynamics of large marine predators, will be presented in a separate paper.

l14 - focus of the paper is on the skill assessment - hence it would be useful to provide a few more quantitative diagnostics both to assess this simulation and allow others to compare their simulations too this model.

Author's response: As detailed above (please see Author's response 6), we added quantitative diagnostics to the revised version.

l15 - very short run, 8 years. Need to convince me the drift in the upper ocean is not significant.
l24 - the short simulation makes the assessment to nutrient and oxygen irrelevant in the deep ocean where the water properties remain similar to initial state. Again some diagnostics of how water properties evolve over the simulation are needed to show they change. This should also be supplement with a quantitative assessment of nutrient simulation in the upper ocean.

Author's response: These points are detailed above; please see Author's response 3

pg4 l19, some additional details of what the physical model does well and not so well would be helpful here.

Author's response:

We ask the reviewer to kindly consider the companion paper by Tranchant et al. It presents a complete evaluation of the physical model.

We added information to the introduction of the revised paper:

“The regional configuration of the ocean dynamics is fully described in Tranchant et al. (this volume, hereafter Part I). The physical model reproduced main processes occurring in this complex oceanic region. Ocean circulation and water mass transformation through the Indonesian Archipelago are close to observations. Eddy Kinetic Energy displays similar patterns to satellite estimates, tides being a dominant forcing in the area. The volume transport of the Indonesian ThroughFlow is comparable to INSTANT data. TS diagrams highlight the erosion of South and North Pacific subtropical waters while crossing the archipelago.”

pg5, line 10, how does the ITF nutrient transports compare to recent estimates? [e.g. Ayers, J. M., Strutton, P. G., Coles, V. J., Hood, R. R. and Matear, R. J.: Indonesian Throughflow nutrient fluxes and their impact on Indian Ocean $\delta^{15}N$ biogeochemistry and productivity, *Geophys. Res. Lett.*, 41(14), 5060–5067, doi:10.1002/2014GL060593, 2014.)

Author's response:

Figure G presents nitrate fluxes at the three exit passages of the ITF (Lombok strait, Ombai strait and Timor passage). Simulated fluxes integrated to the sill depths are compared to Ayers et al. (2014). Negative flux indicates nutrient transport from Indonesian seas to Indian Ocean, while positive flux means a transport from the Indian Ocean back into the Indonesian seas. Simulated fluxes are smaller than estimated ones. Main characteristics are, however, preserved. Across the shallow Lombok strait, the flux is low and towards the Indian Ocean. Across Ombai and Timor straits, nutrient fluxes are seasonally reversed, due to deep currents seasonally directed towards the Indonesian seas while strongest negative fluxes are in the first 300-400m depth (not shown).

A direct comparison of model estimates to Ayers et al. (2014) is not possible for mainly three reasons:

- (1) the INSTANT program took place in 2004-2006, while the simulation started later.
- (2) nitrate flux estimates are sensitive to the position of the currents and the feature of the nitracline. A small shift between modeled and observed features will result in a large bias of modeled fluxes.
- (3) the methodology used by Ayers and coworkers relies on a set of hypothesis hampering a direct comparison with model output.

For all these reasons, we decided against adding the comparison to the revised paper.

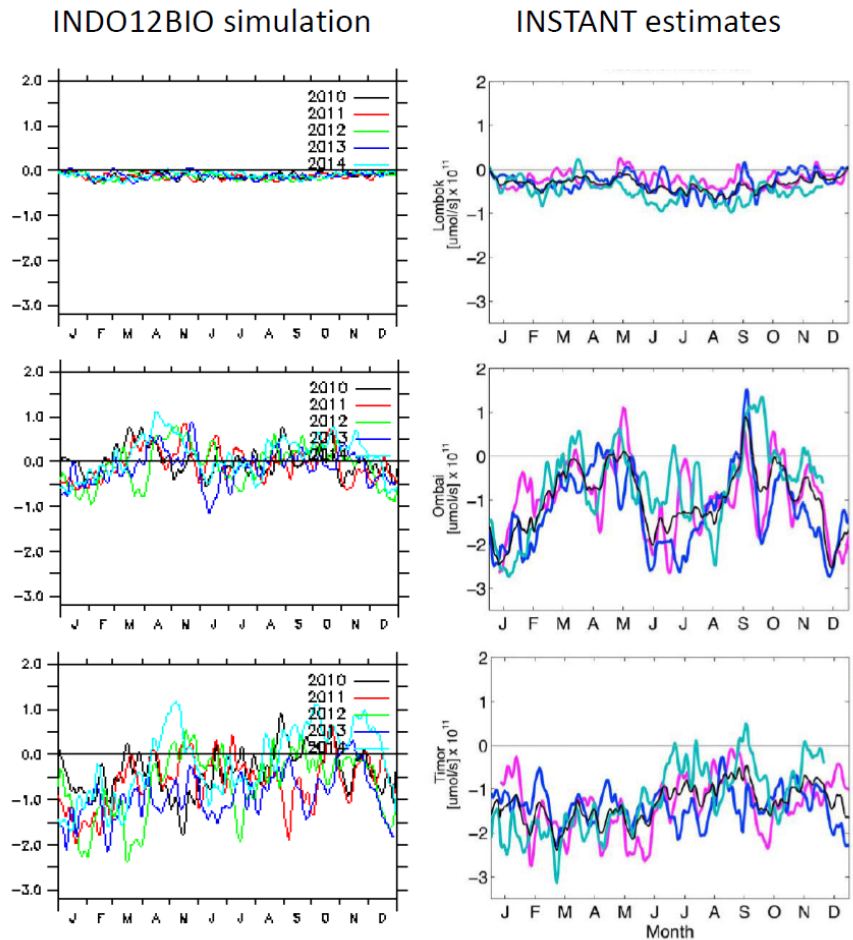


Figure G: Nitrate fluxes integrated to the sill depths, resolved in time (10^{11} $\mu\text{molN/s}$). Top) Lombok 0-300m, middle) Ombai 0-900m, bottom) Timor, 0-1250m. INDO12BIO fluxes (2010-2014) are on the left, INSTANT estimates (2004-2006) on the right.

Pg8 I9, no explicit diffusion - is this just horizontal? isopycnal? Is tidal mixing included?

Author's response:

Vertical diffusion is considered in the advection/diffusion scheme for passive tracers. As mentioned before, the advection scheme (MUSCL) used for the biogeochemical variables is too diffusive. This implicit numerical diffusion is large enough and no additional explicit diffusion is needed. This is a classical feature for numerical simulations using a diffusive advection scheme such as MUSCL. In case a less diffusive advection scheme (i.e. QUICKEST-Zalesak) will be used in future model set-ups, explicit diffusion will have to be taken into account.

Tidal mixing is discussed above (please see Author's response 1).

I16, cite table 1 so it is clear where the initial conditions come from.

Author's response: Yes, it is written in Section 3.2:

"Initial and open boundary conditions are presented in Table 1."

I26, no seasonality to river run-off? This could be a significant issue.

Author's response: This point is already discussed above (please see Author's response 2).

pg 9

I5 the tweaking of sediment loss needs some more justification. For such short run is the increase in nutrient significant? The model may not conserve nutrients since the nutrient transport out of the open boundaries is not necessarily conserved.

I14, short simulation period. You need some additional diagnostics showing how the upper ocean evolves over the simulation. This needs to be plot as a difference from the initial state so enable the changes to be evident in the plot since nutrient display a large vertical gradient that makes it impossible to see how the upper 200 m differs from the observations.

Author's response:

- We agree with the reviewer that the total conservation of nutrients is not expected in a regional configuration due to the open boundaries.

- Concerning the adjustment of nutrient loss to the sediment, it mimics sediment burial of particulate organic carbon. A local equilibrium (at the scale of the regional configuration as opposed to the global ocean) between deposition, burial and remineralization of POC is not a realistic assumption in coastal zones. The small disequilibrium between external inputs and sediment losses allows to compensate for sediment resuspension (e.g. due to tidal forcing) and transport out of the model domain.

- As recommended, additional diagnostics showing how the upper ocean evolves over the simulation are presented in Author's response 3 (see above). The evolution of tracer concentration is presented for the surface, between 0-100m, 100-600m and 600m up to the bottom. Changes can easily be highlighted. The final state can be compared to initial state allowing to appreciate changes. Nutrient, chlorophyll-a, net primary production, sea surface temperature and oxygen concentrations are analyzed. There is no clear temporal trend but rather a vertical adjustment over the length of the simulation. Please refer to Author's response 3 for more details.

I20, you don't just show seasonality much to the assessment.

Author's response: We agree. The evaluation of seasonality has been added to the revised manuscript.

pg12-13 - need to provide a more quantitative assessment for at least chla and nutrients because this would provide a useful benchmark for other model simulations. -some regional numbers would also be useful. What is regional NPP of the model and the observational products?

Author's response: As detailed above (please see Author's response 6), we added additional quantitative diagnostics.

p15l1, hows does the simulated oxygen and nutrient transport through the ITF compare to other estimates?

Author's response: Nutrient transports through ITF exit passages are discussed above.

l8, change "sluggish" to "weak"

Author's response: "sluggish" has been changed to "weak".

pg15, l25, not clear what maximum phase is? change it to month of maximum Chla

Author's response: "maximum phase" has been changed to "month of maximum Chla".

pg 17, l1, model gets the seasonality with no seasonal river input this suggest the rivers are not a important driver of the seasonality.

Author's response: We agree with the reviewer that the model reproduces the large scale seasonality. However, Figures 10 and 11 of the revised manuscript show a lack of temporal correlation between simulated chlorophyll-a and satellite data around the coasts. This weakness hints at the importance of seasonal river inputs of nutrients and carbon.

Comment l20, expand on what the weakness in the model was

Author's response:

We expanded the discussion of the difference between model and observed dissolved Si vertical profiles in the revised version:

"Vertical profiles of nitrate and phosphate are pretty well reproduced, while dissolved Si concentrations are overestimated below 200 m depth. But t should be noted that 2010 is a strong La Niña year and important modifications in the zonal winds, rainfall, river discharges and ocean currents occur. While interannual variations are taken into account in atmospheric forcing and physical open boundary conditions, this is not the case in biogeochemistry. External inputs from rivers are constant, and open boundary conditions come from monthly climatologies. Monthly WOA2009 climatology are close to simulated distributions (not shown), suggesting non-standard conditions during the time of the INDOMIX cruise. "

pg18, some quantitative model data comparison would be useful since this is the focus of the paper.

Author's response: Quantitative numbers are presented in Section 6.

l19, ITF assessment would be useful here.

Author's response: Nutrient transports through the ITF exit passages are discussed above.

l27, focus on sediment BGC but you also do not consider seasonal variability in river run off which also is important. Also the disequilibrium could simply mean the supply of nutrient to the open ocean is required. Perhaps the model is failing in this aspect. It appears the model has too much diffusion of nutrients off shore hence you need to unrealistically increase nutrient remineralization to get the Chla seasonality right. I think this is not a robust result because you lack seasonality to river run off. I think the key point is the coastal nutrient budget needs further development to better reflect the processes like seasonality of nutrient supply, sediment BGC and ocean exchanges. Perhaps having a section on this issue would be helpful since the next paragraph about excessive diffusion is important to getting nutrients off shelf.

Author's response:

We point out the major role of both nutrient supplies: riverine nutrient input and sedimentary processes. Both supplies are discussed in Section 6. Yearly river discharges do not allow the simulation to produce chlorophyll-a maxima along the coasts of Australia and East Sumatra while adding a slight enhancement of water column remineralization leads to higher coastal chlorophyll-a concentrations (Figure H). This slight increase in nutrient remineralization is not unrealistic; it is only a first step to show the importance of sedimentary processes (resuspension and biogeochemistry). While sedimentary processes are required to reproduce chlorophyll-a maxima along the coasts, they do not allow to get the chlorophyll-a seasonality right. This is clearly demonstrated by the poor temporal correlation between the model and the data along the coasts (Please see Figure 11 of the revised paper). Instead monthly river inputs appear key to reproduce observed temporal variations of chlorophyll-a maxima. We point out the crucial role of river run off. Sensitivity tests using the QUICKEST-Zalezak advection scheme (not diffusive) show great impact over the Indonesian archipelago and offshore, but not along the coasts (Figures H and I). Excessive diffusion introduced by MUSCL is not compensated by increased nutrient remineralization. Otherwise, the QUICKEST-Zalezak advection scheme would produce higher chlorophyll-a concentrations along the coasts due to absence of diffusion and increased nutrient remineralization. Both phenomena are decorrelated.

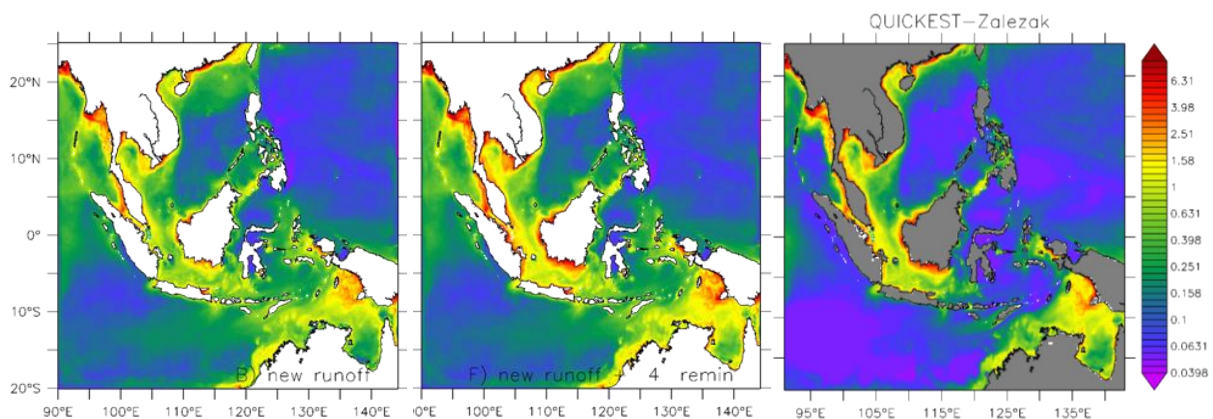


Figure H: Annual mean (year 2010) of surface chlorophyll-a concentrations (mg Chl m^{-3}) with external inputs balanced by sediment losses (left), with + 4% of water column remineralization (middle; corresponding to INDO12BIO configuration), INDO12BIO (+ 4% of water column remineralization) with QUICKEST-Zalezak advection scheme for passive tracers (right).

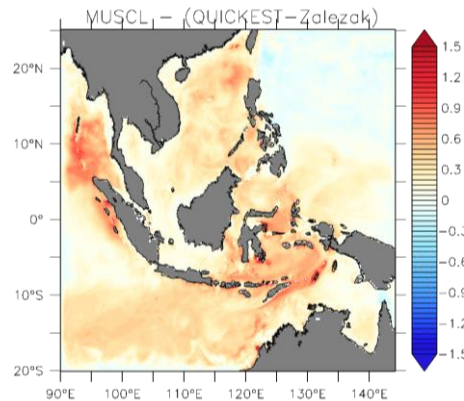


Figure 1: Bias of log-transformed surface chlorophyll-a (MUSCL – QUICKEST Zalezak) for year 2010.

pg19,

I20, how does the regional NPP compare to observations. Does it suggest too much NPP?

Author's response: Quantitative numbers have been included. Yes, they report the overestimation of Chla and NPP in the simulation.

I23-24, sentence has a typo Please summarize what the problems are in the open ocean and why they occur and how they could be improved.

Author's response: The sentence was reformulated: "However, the scheme applies to much pressure on the vertical gradient of nutrients, and the nutricline is considerably strengthened. Hence, before shifting from MUSCL to QUICKEST-Zalezak, model physics needs to be further improved."

This paragraph explains that QUICKEST-Zalezak scheme is better than MUSCL, as it is not diffusive and coherent with model physics. But MUSCL tends towards smoothed fields masking by the way problems of the physics, while QUICKEST-Zalezak accentuates these problems. This implies that the enhancement of the skill of the biogeochemical model through a shift from MUSCL to QUICKEST-Zalezak requires first an improvement of model physics.

I28, how does the open boundary parameterization affect the simulation? No results are discussed to show this impact and the problems it causes.

Author's response:

- The algorithms used for the open boundary conditions are the same than those used for physical tracers (temperature and salinity). They are described in the companion paper by Tranchant et al.

Figure 2 - the most apparent difference is the simulated excessive phytoplankton in the coastal environment. This is interesting because ocean colour often overestimates Chla in these regions because of the contamination by non-chla signal. What does this imply about the model simulation?

Author's response : Indeed, bias (model - MODIS) is almost positive everywhere, with highest values in the coastal environment. This overestimation was discussed above at several occasions (impact of numerical advection scheme, lack of seasonality of river inputs etc.).

Are these coastal region nitrate limited?

Author's response: Please see Author's response 10.

Figure 3. clarify what production model refers to - sum of variance of the 3 different PP models

Author's response: We modified the legend in Figure 5 of the revised manuscript: "Standard deviation of the 3 averaged production models."

Figure 5. It would be useful to know what nutrient is controlling phytoplankton growth. Could you show the surface nitrate, silicate and iron with a scale where it would be easy to distinguish where nutrient limitation is occurring. This would also help answer what is causing the bias in the coastal regions.

Author's response:

For nutrient limitation, please see Author's response 10.

Concerning the bias in the coastal regions, the reason is clearly identified, and already discussed above.

figure 6. dispersion? say it is variability in the data. spread in of WOD in f) does not seem to match averaged value

Author's response:

We modified in Figure 3 of the revised manuscript to: "All the raw data available on each box and gathered in the WOD (light blue crosses) are added in order to illustrate the spread of data."

Simulated dissolved Si in Banda sea (f) matches with WOA and CARS. For WOD, two distinct profiles can be distinguished: one with deep values around 80 mmol Si m³ and a second one close to 140 mmol Si m³. Simulated profile, WOA and CARS profiles match with the second one. So, the question is: why is there two distinct profiles in WOD ? In-situ raw data of WOD can situate in very distinct areas of the Banda box, close to the coast of Sulawesi or Maluku Islands or in the middle of Banda Sea, with distinct hydrodynamical conditions.

Figure 7. Why is there a double peak in the simulation and is this believable? State what you are showing in the maps.

Author's response: The double peak is discussed in Author's response 9.

Figure 8. explain what phase is - timing of the maximum Chl? is so then say this instead.

Author's response: Yes, "phase" means "timing of maximum Chla". We modified this to avoid confusion.

Figure 9. state how normalised sd was estimated

Author's response:

Normalized standard deviation means: standard deviation of the model normalized by the standard deviation of the data.

We clarify this point in the legend: "normalised standard deviation ($\text{std}(\text{model})/\text{std}(\text{data})$) estimated between the INDO12BIO simulation and the MODIS Case-1 ocean colour product."

Figure 10. big difference in f) at 800m. Why? initial state (WOD) is much different the what was observed on the cruise?

Author's response:

There is indeed a big difference in f). This point is discussed in Section 5.4. We added vertical profiles for the climatological month of July for CARS2009 and WOA2009 on Figure J. The CARS profile of dissolved Si is different from of both, INDO12BIO and INDOMIX profiles, while WOA is closer to INDO12BIO. However, the vertical profile measured during the INDOMIX cruise stands out, especially between 400 and 1000 m. The INDOMIX cruise took place during a La Niña year and we hypothesize that corresponding strong modifications in the zonal winds, rainfall, river discharges and ocean currents could explain the peculiar shape of profile.

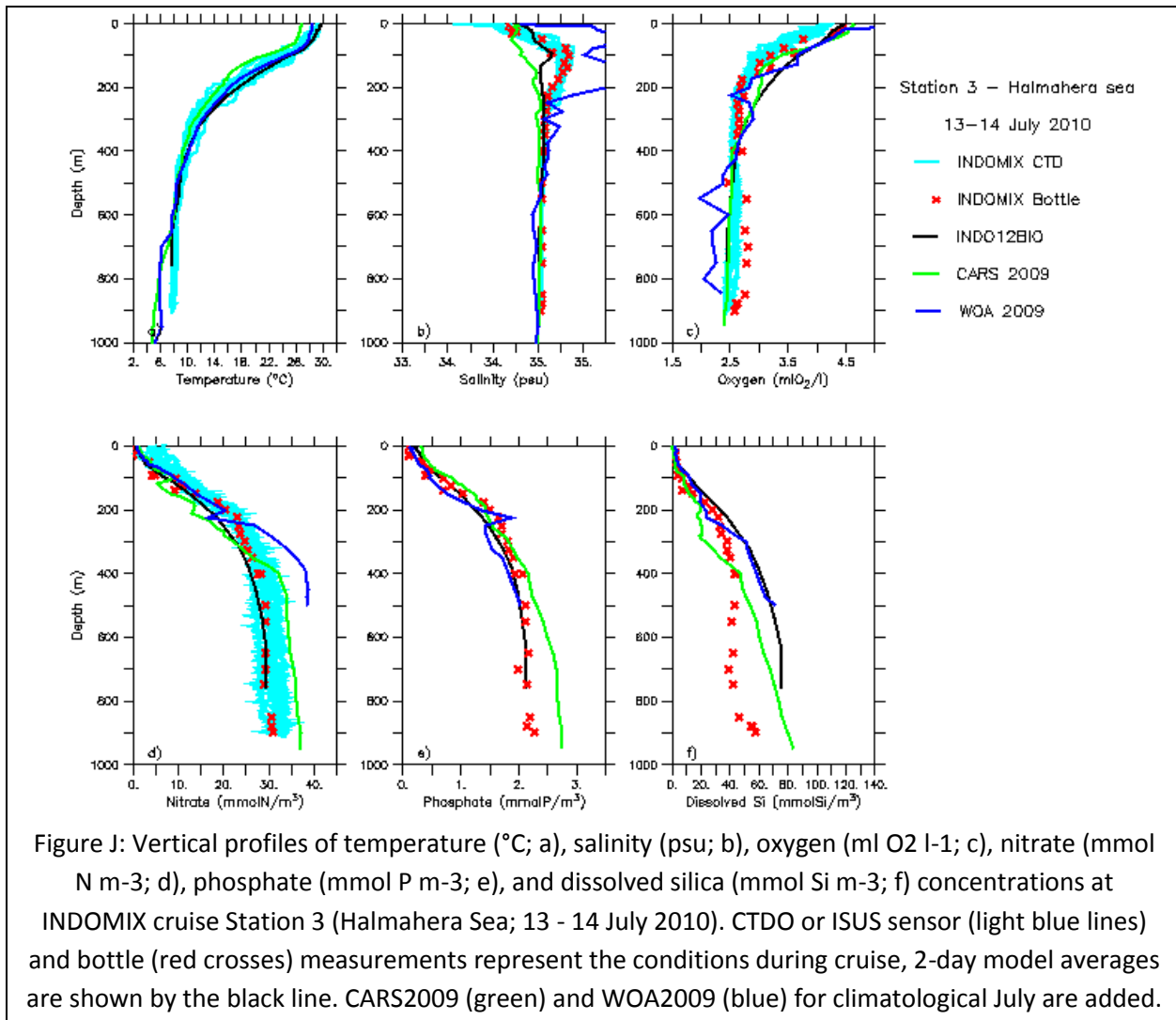


Figure J: Vertical profiles of temperature (°C; a), salinity (psu; b), oxygen (ml O₂ l⁻¹; c), nitrate (mmol N m⁻³; d), phosphate (mmol P m⁻³; e), and dissolved silica (mmol Si m⁻³; f) concentrations at INDOMIX cruise Station 3 (Halmahera Sea; 13 - 14 July 2010). CTDO or ISUS sensor (light blue lines) and bottle (red crosses) measurements represent the conditions during cruise, 2-day model averages are shown by the black line. CARS2009 (green) and WOA2009 (blue) for climatological July are added.

Evaluation of an operational ocean model configuration at 1/12° spatial resolution for the Indonesian seas (NEMO2.3/INDO12). Part II: Biogeochemistry

E. Gutknecht¹, G. Reffray¹, M. Gehlen², I. Triyulianti³, D. Berlianty³, and P. Gaspar⁴

[1]{Mercator Océan, 8-10 rue Hermès, 31520 Ramonville, France}

[2]{LSCE, UMR CEA-CNRS-UVSQ, Saclay, L'Orme des Merisiers, 91191 Gif-sur-Yvette, France}

[3]{Institute for Marine Research and Observation, Jl. Baru Perancak, Negara-Jembrana, Bali 82251, Republic of Indonesia}

[4]{CLS, 8-10 rue Hermès, 31520 Ramonville, France}

Correspondence to: E. Gutknecht (elodie.gutknecht@mercator-ocean.fr)

Abstract

In the framework of the INDES0 (Infrastructure Development of Space Oceanography) project, an operational ocean forecasting system was developed to monitor the state of the Indonesian seas in terms of circulation, biogeochemistry and fisheries. This forecasting system combines a suite of numerical models connecting physical and biogeochemical variables to population dynamics of large marine predators (tunas). The physical/biogeochemical coupled component (the INDO12BIO configuration) covers a large region extending from the western Pacific Ocean to the Eastern Indian Ocean at 1/12° horizontal resolution. The OPA/NEMO physical ocean model and the PISCES biogeochemical model are coupled in “on-line” mode without degradation in space and time. The operational global ocean forecasting system (1/4°) operated by Mercator Ocean provides the physical forcing, while climatological open boundary conditions are prescribed for the biogeochemistry.

This paper describes the skill assessment of the INDO12BIO configuration. Model skill is assessed by evaluating a reference hindcast simulation covering the last 8 years (2007-2014).

Model results are compared to satellite, climatological and in-situ observations. Diagnostics are performed on chlorophyll-a, primary production, mesozooplankton, nutrients and oxygen.

The model reproduces large scale distributions of nutrients, oxygen, chlorophyll-a, NPP and mesozooplankton biomasses. Modelled vertical distributions of nutrients and oxygen are comparable to in-situ datasets although gradients are slightly smoothed. The model simulates realistic biogeochemical characteristics of North Pacific tropical waters entering in the archipelago. Hydrodynamics transformation of water masses across the Indonesian archipelago allows conserving nitrate and oxygen vertical distribution close to observations, in the Banda Sea and at the exit of the archipelago. While the model overestimates the mean surface chlorophyll-a, the seasonal cycle is in phase with satellite estimations, with higher chlorophyll-a concentrations in the southern part of the archipelago during SE monsoon, and in the northern part during NW monsoon. The time-series of chlorophyll-a anomalies suggests that meteorological and ocean physical processes that drive the interannual variability of biogeochemical properties in the Indonesian region are reproduced by the model.

Introduction

The “Coral triangle” delineated by Malaysia, the Philippines, New Guinea, Solomon Islands, East-Timor and Indonesia is recognized as a global hotspot of marine biodiversity (Allen and Werner, 2002; Mora et al., 2003; Green and Mous, 2004; Allen, 2008). It gathers 20% of the world’s species of plants and animals, and the greatest concentration and diversity of reefs (76% of the world’s coral species; Veron et al., 2009). The Indonesian archipelago is located at the centre of this ecologically rich region. It is characterized by a large diversity of coastal habitats such as mangrove forests, coral reefs and sea grass beds, all of which shelter ecosystems of exceptional diversity (Allen and Werner, 2002). The archipelago's natural heritage represents an important source of income and employment, with its future critically depending on the sustainable management of ecosystems and resources (e.g. Foale et al., 2013; Cros et al., 2014).

The wider Coral Triangle and its sub-region, the Indonesian archipelago, are facing multiple threats resulting from demographic growth, economic development, change in land use

practices and deforestation, as well as global climate change (<http://www.metoffice.gov.uk/media/pdf/8/f/Indonesia.pdf> ; FAO, 2007). Human activities cause changes in the delivery of sediments, nutrients and pollutants to coastal waters, leading to eutrophication, ecosystem degradation, as well as species extinctions (Ginsburg, 1994; Pimentel et al., 1995; Bryant et al., 1998; Roberts et al., 2002; UNEP, 2005; Alongi et al., 2013). Surveys report an over 30% reduction of mangroves in Northern Java over the last 150 years and an increase of coral reef degradation from 10% to 50% in the last 50 years (Bryant et al., 1998; Hopley and Suharsono, 2000; UNEP, 2009), leading to 80% of the reefs at risk in this region (Bryant et al., 1998). These changes not only damage coastal habitats, but also propagate across the whole marine ecosystem from nutrients and the first levels of the food web up to higher trophic levels, along with concomitant changes in biogeochemical cycles.

There is thus a vital need for monitoring and forecasting marine ecosystem dynamics. The INDESO project (Infrastructure Development of Space Oceanography, www.indeso.web.id/indeso_wp/index.php), funded by the Indonesian Ministry of Marine Affairs and Fisheries, aims at the development of sustainable fishery practices in Indonesia, the monitoring of its Exclusive Economic Zone (EEZ) and the sustainable management of its ecosystems. The project addresses the Indonesian need for building a national capability for operational oceanography. The model system consists of three models deployed at the scale of the Indonesian archipelago: an ocean circulation model (NEMO-OPA; Madec , 2008), a biogeochemical model (PISCES; Aumont and Bopp, 2006) with a spatial resolution of 1/12°, as well as an intermediate trophic level/fish population dynamics model (SEAPODYM; Lehodey et al, 2008). Since mid-September 2014, the chain of models is fully operational in Perancak (Bali, Indonesia) and delivers 10-day forecast / two weeks hindcast on a weekly basis (see <http://www.indeso.web.id>).

The regional configuration of ocean dynamics is fully described in Tranchant et al. (this volume, hereafter Part I). The physical model reproduces main processes occurring in this complex oceanic region. Ocean circulation and water mass transformation through the Indonesian Archipelago are close to observations. Eddy Kinetic Energy displays similar patterns to satellite estimates, tides being a dominant forcing in the area. The volume transport of the Indonesian ThroughFlow is comparable to INSTANT data. TS diagrams highlight the erosion of South and North Pacific subtropical waters while crossing the archipelago.

The present paper (Part II) focuses on ocean biogeochemistry. It is organized as follows. The next section presents an overview of the area of study with emphasis on main drivers of

biological production over the Indonesian archipelago. The biogeochemical component of the physical-biogeochemical coupled configuration is described in Section 3. Satellite, climatological and *in-situ* observations used to evaluate simulation results are detailed in Section 4. Section 5 presents the evaluation of the skill of the coupled model to reproduce main biogeochemical features of Indonesian seas along with their seasonal dynamics (Section 5). Finally, discussion and conclusion are presented in Section 6.

Area of study

The Indonesian archipelago is crossed by North and South Pacific waters that converge in the Banda Sea, and leave the archipelago through three main straits: Lombok, Ombai and Timor. This ocean current (Indonesian ThroughFlow; ITF) provides the only low-latitude pathway for warm, fresh waters to move from the Pacific to the Indian Ocean (Gordon, 2005; Hirst and Godfrey, 1993). On their way through the Indonesian archipelago, water masses are progressively transformed by surface heat and freshwater fluxes and intense vertical mixing linked to strong internal tides trapped in the semi-enclosed seas as well as upwelling processes (Field and Gordon, 1992). The main flow, as well as the transformation of Pacific waters is correctly reproduced by the physical model, with a realistic distribution of the volume transport through the three major outflow passages (part I). In the Indian Ocean, this thermocline water mass forms a cold and fresh tongue between 10°S and 20°S, and supplies the Indian Ocean with nutrients. These nutrients impact biogeochemical cycles and support new primary production in the Indian Ocean (Ayers et al., 2014).

Over the archipelago, complex meteorological and oceanographic conditions drive the distribution and growth of phytoplankton and provide favourable conditions for the development of a diverse and productive food web extending from zooplankton, and intermediate trophic levels to pelagic fish (Hendiarti et al., 2004, 2005; Romero et al., 2009). The tropical climate is characterized by a monsoon regime and displays a well-marked seasonality. The south-east (SE) monsoon (April to October) is associated with easterlies from Australia that carry warm and dry air over the region. Wind-induced upwelling along the southern coasts of Sumatra, Java and Nusa-Tenggara Islands (hereafter named Sunda Islands) and in the Banda Sea is associated with high chlorophyll-*a* levels (Susanto et al., 2006; Rixen et al., 2006). Chlorophyll-*a* maxima along Sunda Islands move to the west over the period of the SE monsoon, in response to the alongshore wind shift and associated movement of the upwelling centre (Susanto et al., 2006). From October to April, the northwest (NW) monsoon

is associated with warm and moist winds from the Asian continent. Winds blow in a southwest direction north of the Equator and towards Australia south of the Equator. They generate a downwelling and a reduced chlorophyll-*a* content south of the Sunda Islands and in the Banda Sea. The NW monsoon also causes some of the highest precipitation rates in the world. Increased river runoff carries important sediment loads (20 to 25% of the global riverine sediment discharge; Milliman et al., 1999), along with carbon and nutrients to the ocean. These inputs are a strong driver of chlorophyll-*a* variability and play a key role in modulating the biological carbon pump across Indonesian seas (Hendiarti et al., 2004; Rixen et al., 2006). High levels of suspended matter decrease the water transparency in coastal areas and modify the optical properties of waters which in turn interferes with ocean colour remote sensing (Susanto et al., 2006). Although several Indonesian rivers are classified among the 100 most important rivers of the world, most of them are not regularly monitored. It is thus currently impossible to estimate the impact of river runoff on the variability of chlorophyll-*a* in the region (Susanto et al., 2006).

Indonesian seas are also greatly influenced by modes of natural climate variability owing to its position on the equator between Asia and Australia and between the Pacific and Indian oceans. Strength and timing of the seasonal monsoon are modulated by interannual phenomena that disturb atmospheric conditions and ocean currents. A significant correlation between the variability of the Indonesian ThroughFlow (ITF) and the El Niño-Southern Oscillation (ENSO) was reported (e.g. Meyers, 1996; Murtugudde et al., 1998; Potemra et al., 1997), with ENSO modulating rainfall and chlorophyll-*a* on inter-annual timescales (Susanto et al., 2001, 2006; Susanto and Marra, 2005). In the eastern Indian Ocean, large anomalies off Sumatra and Java coasts are associated with the Indian Ocean Dipole (IOD) Mode monitored via the Dipole Mode Index (DMI; Saji et al., 1999). A strong positive index points to abnormally strong coastal upwelling and a large phytoplankton bloom near Java Island (Meyers, 1996; Murtugudde et al., 1999). Inside the archipelago, effects of each climate mode are more difficult to analyse as both influence ITF transport. There is, however, evidence for Indian Ocean dynamics to dominate over Pacific Ocean dynamics as drivers of ITF transport variability (Masumoto, 2002; Sprintall and Révelard, 2014).

Finally, tides, the Madden-Julian Oscillation, Kelvin and Rossby waves are additional drivers of variability across Indonesian seas and influence marine ecosystems (Madden and Julian, 1994; Field and Gordon, 1996; Sprintall et al., 2000; Susanto et al., 2000, 2006).

The INDO12BIO configuration

The coupled model

In the framework of the INDES0 project, a physical-biogeochemical coupled model is deployed over the domain from 90°E-144°E to 20°S-25°N, widely encompassing the whole Indonesian archipelago, with a spatial resolution of 1/12°. The physical model is based on the NEMO-OPA 2.3 circulation model (Madec et al., 1998; Madec, 2008). Specific improvements include time-splitting and non-linear free surface to correctly simulate high frequency processes such as tides. A parameterization of the vertical mixing induced by internal tides has especially been developed for NEMO-OPA (Koch-Larrouy et al., 2007, 2010) and is used here. The physical configuration called INDO12 is described in detail in Part I (Tranchant et al., this volume).

Dynamics of biogeochemical properties across the area are simulated by the PISCES model version 3.2 (Aumont and Bopp, 2006). PISCES simulates the first levels of the marine food web from nutrients up to mesozooplankton. It has 24 state variables. PISCES considers five limiting nutrients for phytoplankton growth (nitrate and ammonium, phosphate, dissolved Si and iron). Four living size-classified compartments are represented: two phytoplankton groups (nanophytoplankton and diatoms) prognostically predicted in C, Fe, Si (the latter only for diatoms) and chlorophyll content, and two zooplankton groups (microzooplankton and mesozooplankton). Constant C/N/P Redfield ratios are supposed for all species. While internal Fe/C and Si/C ratios of phytoplankton are modelled as a function of the external availability of nutrients and thus variable, only C is prognostically modelled for zooplankton. The model includes five non-living compartments: small and big particulate organic carbon and semi-labile dissolved organic carbon, particulate inorganic carbon (CaCO₃ as calcite) and biogenic silica. PISCES also simulates Dissolved Inorganic Carbon (DIC), total alkalinity (carbonate alkalinity + borate + water), and dissolved oxygen. The CO₂ chemistry is computed following the OCMIP protocols (<http://ocmip5.ipsl.jussieu.fr/OCMIP/>). Biogeochemical parameters are based on the standard PISCES namelist version 3.2. Please refer to Aumont and Bopp (2006) for a comprehensive description of the model (v3.2).

PISCES is coupled to NEMO-OPA via the TOP component that manages the advection/diffusion equations of passive tracers and biogeochemical source and sink terms. In our regional configuration, called INDO12BIO, physics and biogeochemistry are running simultaneously (“on-line” coupling), at the same resolution. Particular attention must be paid

to respect a number of fundamental numerical constraints. 1/ The numerical scheme of PISCES for biogeochemical processes is forward in time (Euler), which does not correspond to the classical leap-frog scheme used for the physical component. Moreover, the free surface explicitly solved by the time splitting method is non linear. In order to respect the conservation of the tracers, the coupling between biogeochemical and physical components is done every second time step. As a result, the biogeochemical model is controlled by only one leap-frog trajectory of the dynamical model. The use of an asselin filter allows keeping the two numerical trajectories close enough to overcome this shortcoming. The advantage is a reduction of numerical cost and a time step for the biogeochemical model twice that of the physical component ie. 900 seconds. 2/ As this time step is small, no time-splitting was used in the sedimentation scheme. 3/ The advection scheme is the standard scheme of TOP-PISCES ie. the Monotonic Upstream centered Scheme for Conservation Laws (MUSCL) (Van Leer, 1977). No explicit diffusion has been added as the numerical diffusion introduced by this advection scheme is already important.

Initial and open boundary conditions

The simulation starts on January 3rd, 2007 from the global ocean forecasting system at 1/4° operated by Mercator-Ocean (PSY3 described in Lellouche et al., 2013) for temperature, salinity, currents, and free surface at the same date. Open boundary conditions (OBC) are also provided by daily outputs of this system. A 1° thick buffer layer allows nudging the signal at the open boundaries.

Initial and open boundary conditions are derived from climatological data sets for nitrate, phosphate, dissolved Si, oxygen, dissolved inorganic carbon, and alkalinity. For tracers for which this information is missing, initial and open boundary conditions come either from a global scale simulation, or they have to be estimated from satellite data, respectively build using analytical values. The global scale model NEMO-OPA/PISCES has been integrated for 3000 years at 2° horizontal resolution, until PISCES reached a quasi steady-state (see Aumont and Bopp, 2006). A monthly climatology was built for dissolved iron and DOC based on this simulation. Initial and open boundary conditions are summarized in Table 1. A Dirichlet boundary condition is used to improve the information exchange between the OBC and the interior of the domain.

External inputs

Three different sources are supplying the ocean in nutrients: atmospheric dust deposition, sediment mobilization, and rivers. Atmospheric deposition of iron comes from the climatological monthly dust deposition simulated by the model of Tegen and Fung (1995), and that of Si follows Moore et al. (2002). Yearly river mean discharges are taken from the Global Erosion Model (GEM) of Ludwig et al. (1996) for DIC, and from the Global News 2 climatology (Mayorga et al., 2010) for nutrients. An iron source corresponding to sediment reductive mobilization on continental margins is also considered. For more details on external supply of nutrients, please refer to the supplementary material of Aumont and Bopp (2006). In PISCES, external input fluxes are compensated by a loss to the sediments as particulate organic matter, biogenic Si and CaCO₃. These fluxes correspond to matter definitely lost from the ocean system. The compensation of external input fluxes through output at the lower boundary closes the mass balance of the model. While such an equilibrium is a valid assumption at the scale of the global ocean, it is not reached at regional scale. For the INDO12BIO configuration, a decrease of the nutrient and carbon loss to the sediment was introduced corresponding to an increase in the water column remineralization by ~4%. This slight enhancement of water column remineralization leads to higher coastal chlorophyll-*a* concentrations (about +1 mg Chl m⁻³) and enables the model to reproduce the chlorophyll-*a* maxima observed along the coasts of Australia and East Sumatra (not shown).

Simulation length

The simulation started on January 3rd, 2007 and operates up to present day as the model currently delivers ocean forecasts. For the present paper, we will analyse the simulation up to December 31, 2014. The spin-up length depends on the biogeochemical tracer (Fig. 1). The total carbon inventory computed over the domain (defined as the sum of all solid and dissolved organic and inorganic carbon fractions, yet dominated by the contribution of DIC) equilibrates within several months. To the contrary, Dissolved Organic Carbon (DOC), phosphate (PO₄) and Iron (Fe) need several years to stabilize (Fig. 1). The annual mean for year 2011 is used for comparison to satellite products (chlorophyll-*a*, primary production). For comparison to climatologies (zooplankton, nutrients, oxygen) and analysis of the seasonal cycle, we are using years 2010 to 2014. Interannual variability is assessed over the whole length of simulation except the first year (2008 to 2014).

Satellite, climatological and *in-situ* data

Model outputs are compared to satellite, climatological, and *in-situ* observations. These observational data are detailed and described in this section.

INDOMIX cruise

The INDOMIX cruise on-board Marion Dufresne RV (Koch-Larrouy et al., in revision) crossed the Indonesian archipelago between the 09th and 19th of July 2010, and focused on one of the most energetic sections for internal tides from Halmahera Sea to Ombai Strait. Repeated CTD profiles over 24 hours as well as measurements of oxygen and nutrients were obtained for six stations at the entrance of the archipelago (Halmahera Sea), in the Banda Sea and in the Ombai Strait (three of them are used for validation; cf stations on Fig. 4). This data set provides an independent assessment of model skill. To co-localise model and observations, we took the closest simulated point to the coordinates of the station. 2-day model averages were considered as measurements were performed during 2 consecutive days at the stations selected for validation.

Nutrients and Oxygen

Modelled nutrient and oxygen distributions are compared to climatological fields of World Ocean Atlas 2009 (WOA 2009, 1° spatial resolution) (Garcia et al., 2010a, 2010b), respectively, the CSIRO Atlas of Regional Seas 2009 (CARS 2009, 0.5° spatial resolution) and discreet observations provided by the World Ocean Database 2009 (WOD 2009) Only nitrate, dissolved Si and oxygen distributions are presented hereafter. Nitrate + ammonium and phosphate are linked by a Redfield ratio in PISCES.

Chlorophyll-a

The ocean colour signal reflects a combination of chlorophyll-*a* content, suspended matter, coloured dissolved organic matter (CDOM) and bottom reflectance. Singling out the contribution of phytoplankton's chlorophyll-*a* is not straightforward in waters for which the relative optical contribution of the three last components is significant. This is the case over vast areas of the Indonesian archipelago where river discharges and shallow water depths contribute to optical properties (Susanto et al., 2006). The interference with optically absorbing constituents other than chlorophyll-*a* results in large uncertainties in coastal waters (up to 100%, as compared to 30% for open ocean waters) (Moore et al., 2009). Standard

algorithms distinguish between open ocean waters / clear waters (Case-1) and coastal waters / turbid waters (Case-2). The area of deployment of the model comprises waters of both categories and the comparison between modelled chlorophyll-*a* and estimates derived from remote sensing can be only qualitative. Two single mission monthly satellite products are used for model skill evaluation. MODIS-Aqua (EOS mission, NASA) Level-3 Standard Mapped Image product (NASA Reprocessing 2013.1) covers the whole simulated period (2007-2014). It is a product for Case-1 waters, with a 9 km resolution, and is distributed by the ocean colour project (<http://oceancolor.gsfc.nasa.gov/cms/>). The MERIS (ENVISAT, ESA) L3 product (ESA 3rd reprocessing 2011) is also considered. Its spectral characteristics allow the use of an algorithm for Case-2 waters (MERIS C2R Neural Network algorithm; Doerffer and Schiller, 2007). It has a 4 km resolution and is distributed by ACRI-ST (<http://www.acri-st.fr/>), unfortunately the mission ended in April 2012.

Net primary production

Net primary production (NPP) is at the base of the food-chain. *In situ* measurements of primary production are sparse and we rely on products derived from remote sensing for model evaluation. The link between pigment concentration (chlorophyll-*a*) and carbon assimilation reflects the distribution of chlorophyll-*a* concentrations, but also the uncertainty associated to the production algorithm and the ocean colour product. At present, the community uses three production models. The Vertically Generalized Production Model (VGPM) (Behrenfeld and Falkowski, 1997) estimates NPP as a function of chlorophyll, available light, and photosynthetic efficiency. It is currently considered as the Standard algorithm. The two alternative algorithms are an "Eppley" version of the VGPM (distinct temperature-dependent description of photosynthetic efficiencies) and the Carbon-based Production Model (CbPM; Behrenfeld et al. 2005, Westberry et al. 2008). The latter estimates phytoplankton carbon concentration from remote sensing of particulate scattering coefficients. Henson et al. (2010) point to the uncertainty of the CbPM algorithm, which yields results that are substantially different from the other algorithms. However, Emerson (2014) recommends the CbPM algorithm for providing the best results when tested at three time series sites (BATS, HOTS and OSP stations). A complete description of the products is available at www.science.oregonstate.edu/ocean.productivity. Here we compare the simulated NPP to NPP derived from the three production models using MODIS ocean colour estimates.

Mesozooplankton

MAREDAT, MARine Ecosystem DATA (Buitenhuis et al., 2013), is a collection of global biomass datasets for major plankton functional types (e.g. diatoms, microzooplankton, mesozooplankton etc.). Mesozooplankton is the only MAREDAT field covering the Indonesian archipelago. The database provides monthly fields at a spatial resolution of 1°. Mesozooplankton data are described in Moriaty and O'Brien (2013). Samples are taken with a single net towed over a fixed depth interval (e.g. 0-50m, 0-100m, 0-150m, 0-200m...) and represent the average population biomass ($\mu\text{g C l}^{-1}$) throughout a depth interval. For this study, only annual mean mesozooplankton biomasses are used. Monthly fields have a too sparse spatial coverage over the Indonesian archipelago and represent different years. It is thus not possible to extract a seasonal cycle.

INDO12BIO Evaluation

The ability of the INDO12BIO coupled physical-biogeochemical model to reproduce the observed spatial distribution and temporal variability of biogeochemical tracers is assessed for nutrients and oxygen concentrations, chlorophyll-*a*, net primary production (NPP), and mesozooplankton biomass. Model evaluation focuses on annual mean state, mean seasonal cycle, and interannual variability. It is completed by a comparison between model output and data from the INDOMIX cruise.

Annual mean state

Nutrients and Oxygen

Nitrate and oxygen distributions at 100 m depth are presented on Fig. 2 for CARS, WOA and the model. Dissolved Si has the same distribution as nitrate (not shown). The marked meridional gradient seen in observations of the Pacific and Indian Oceans, is correctly reproduced by the model. Low nitrate and high oxygen concentrations in the subtropical gyres of the North Pacific and South Indian Oceans are due to Ekman-induced downwelling. Higher nitrate and lower oxygen concentrations in the equatorial area are associated with upwelling. Maxima nitrate concentrations associated with minima oxygen concentrations are noticeable in the Bay of Bengal and Adaman Sea (north of Sumatra and west of Myanmar). They reflect discharges by major rivers (Brahmaputra, Ganges and other river systems) and associated increase in oxygen demand. Low nitrate and high oxygen concentrations at 100 m depth in the

Sulawesi Sea reflect the signature of Pacific waters entering in the archipelago, a feature correctly reproduced by the model. The signature slowly disappears as waters progressively mix along their pathways across the archipelago. The resulting higher nitrate and lower oxygen levels at 100 m depth in the Banda Sea are reproduced by the model. Higher nitrate and lower oxygen concentrations off the Java-Nusa-Tenggara island chain in data and model output reflect seasonal alongshore upwelling.

To evaluate the vertical distribution of simulated nutrient and oxygen concentrations over the Indonesian archipelago, vertical profiles of oxygen, nitrate and dissolved Si are compared to climatologies provided by CARS and WOA, as well as to discrete data from WOD (Fig. 3). Vertical profiles are analysed in key areas for the Indonesian ThroughFlow (Koch-Larrouy et al., 2007): (1) one box in the North Pacific Ocean, which is representative of water masses entering the archipelago, (2) one box in the Banda Sea where Pacific waters are mixed to form the ITF, and (3) one box at the exit of the Indonesian archipelago (Timor Strait). Biogeochemical characteristics of tropical Pacific water masses entering the archipelago are correctly reproduced by the model (Fig. 3). The flow across the Indonesian archipelago and the transformation of water masses simulated by the model result in realistic vertical distributions of nutrients and oxygen concentrations in the Banda Sea. The ITF leaves the archipelago and spreads into the Indian Ocean with a biogeochemical content in good agreement with the data available in the area.

However, simulated vertical structures are slightly smoothed compared to data (Fig. 3). The vertical gradient of nitrate is too weak over the first 2000m depth of the water column (North Pacific and Timor), and the area of minima oxygen concentrations is eroded (especially in North Pacific box). This bias is even more pronounced on the vertical gradient of dissolved Si (Fig. 3). The smoothing of vertical structures results from the numerical advection scheme MUSCL currently used in PISCES, which is known to be too diffusive (Lévy et al., 2001).

Chlorophyll-a and NPP

The simulation reproduces the main characteristics of the large scale distribution of chlorophyll-a, a proxy of phytoplankton biomass (Fig. 4). Pacific and Indian subtropical gyres are characterized by low concentrations due to gyre-scale downwelling and hence a deeper nutricline. Highest concentrations are simulated along the coasts driven by riverine nutrient supply, sedimentary processes, as well as upwelling of nutrient-rich deep waters. In comparison to the Case-1 ocean colour product, the model overestimates the chlorophyll-a

content on oligotrophic gyres and the cross-shore gradient is too weak. As a result, the mean chlorophyll-*a* concentration over the INDO12BIO domain is higher in the simulation ($0.53 \text{ mg Chl m}^{-3}$ with a spatial standard deviation of $0.92 \text{ mg Chl m}^{-3}$ over the domain) compared to MODIS ($0.3 \pm 0.74 \text{ mg Chl m}^{-3}$). The bias (as model - observation) is almost positive everywhere, except around the coasts (discussed later) and in the Sulawesi sea. As mentioned in the preceding section, optical characteristics of waters over the Indonesian archipelago are closer to Case-2 waters (Moore et al., 2009). Simulated chlorophyll-*a* concentrations are indeed closer to those derived with an algorithm for Case-2 waters (MERIS) and its mean value of $0.48 \pm 1.4 \text{ mg Chl m}^{-3}$.

The model reproduces the spatial distribution, as well the rates of NPP over the model domain (Fig. 5). However, as mentioned before, NPP estimates depend on the primary production model (in this case, VGPM, CbPM, and Eppley) and on the ocean colour data used in the production models. For a single ocean colour product (here MODIS), NPP estimates display a large variability (Fig. 5). Mean NPP over the INDO12BIO domain is $34.5 \text{ mmol C m}^{-2} \text{ d}^{-1}$ for VGPM with a standard deviation over the domain of $33.8 \text{ mmol C m}^{-2} \text{ d}^{-1}$, $40.4 \pm 22 \text{ mmol C m}^{-2} \text{ d}^{-1}$ for CbPM and $55 \pm 52.7 \text{ mmol C m}^{-2} \text{ d}^{-1}$ for Eppley. NPP estimates from VGPM are characterized by low rates in the Pacific ($<10 \text{ mmol C m}^{-2} \text{ d}^{-1}$) and a well marked cross-shore gradient. The use of CbPM results in low coastal NPP and almost uniform rates over a major part of the domain and including the open ocean (Fig. 5). The Eppley production model is the most productive one with rates about $15 \text{ mmol C m}^{-2} \text{ d}^{-1}$ in the Pacific and higher than $300 \text{ mmol C m}^{-2} \text{ d}^{-1}$ in the coastal zone. The large uncertainty associated with these products precludes a quantitative evaluation of modelled NPP. Like for chlorophyll-*a*, modelled NPP falls within the range of remote sensing derived estimates, with maybe a too weak cross-shore gradient inherited from the chlorophyll-*a* field. The mean NPP over the INDO12BIO domain is, however, overestimated ($61 \pm 41.8 \text{ mmol C m}^{-2} \text{ d}^{-1}$).

Mesozooplankton

Mesozooplankton link the first level of the marine food web (primary producers) to the mid- and, ultimately, high trophic levels. Modelled mesozooplankton biomass is compared to observations in Fig. 6. While the model reproduces the spatial distribution of mesozooplankton, it overestimates biomass by a factor 2 or 3. This overestimation is likely linked to the above-described overestimation of chlorophyll-*a* and NPP.

Mean seasonal cycle

The monsoon system drives the seasonal variability of chlorophyll-a over the area of study. Northern and southern parts of the archipelago exhibit a distinct seasonal cycle (Fig. 7, 8 and 9). In the southern part, the highest chlorophyll concentrations occur from June to September (Banda Sea and Sunda area in Fig. 8 and 9) due to upwelling of nutrient-rich waters off Sunda Islands and in the Banda Sea triggered by alongshore south-easterly winds during SE monsoon. The decrease in chlorophyll levels during NW monsoon is the consequence of north-westerly winds and associated downwelling in these same areas. In the northern part, high chlorophyll concentrations occur during NW monsoon (South China Sea in Fig. 7) when moist winds from Asia cause intense precipitations. A secondary peak is observed during NW monsoon in the southern part and during SE monsoon in the northern part due to meteorological and oceanographic conditions described above.

The annual signal of chlorophyll-a in each grid point gives a synoptic view of the effect of the Asia-Australia monsoon system on the Indonesian archipelago. A harmonic analysis is applied on the time series of each grid point to extract the annual signal in model output and remote sensing data (MODIS). The results of the annual harmonic analysis are summarized in Fig. 10 and highlight the month of maximum chlorophyll-a and the amplitude of the annual signal. The timing of maximum chlorophyll-a presents a north-south distribution in agreement with the satellite observations. The simulation reproduces the chlorophyll-a maxima in July in the Banda Sea and off the south coasts of Java-Nusa-Tenggara. Consistent with observations, simulated chlorophyll-a maxima move to the west over the period of the SE monsoon, in response to the alongshore wind shift. North of the Nusa-Tenggara Islands, maxima in January-February are due to upwelling associated with alongshore north-westerly winds. In the South China Sea, maxima spread from July-August in the western part (off Mekong River) and gradually shift up to January-February in the eastern part.

The temporal correlation between modelled chlorophyll-a and estimates derived from remote sensing is 0.55 over the entire INDO12BIO domain, but reaches 0.78 in the South China sea, 0.8 in the Banda Sea and 0.92 in the Indian Ocean (Fig. 7, 8, 9 and 11). These high correlation coefficients are associated with low normalized standard deviations (close to 1) in the Banda Sea and in the Indian Ocean (Fig. 11) and large amplitudes in simulated and observed chlorophyll-a (Fig. 10). Normalized standard deviations are higher in the South-East China Sea, Java and Flores Seas, but also in the open ocean due to larger amplitudes in simulated chlorophyll-a. The offshore spread of the high amplitude reflects the too weak cross-shore

gradient of simulated chlorophyll-a (Section 5.1.2), and leads to an increase of the normalized standard deviation with the distance to the coast. For semi-enclosed seas, however, this result has to be taken with caution as clouds cover these regions almost 50-60% of the time period.

The model does not succeed in simulating chlorophyll-a variability in the Pacific sector (Fig. 10 and 11). This area is close to the border of the modelled domain and is influenced by the OBCs derived from the global operational ocean general circulation model. Analysis of the modelled circulation (part I) highlights the role of OBCs in maintaining realistic circulation patterns in this area, which is influenced by the equatorial current system. Part I points, in particular, to the incorrect positioning of Halmahera and Mindanao eddies in the current model, which contributes to biases in simulated biogeochemical fields.

Finally, correlation is low close to the coasts and the temporal variability of the model is lower than that of the satellite product, with normalized standard deviation < 1 (Fig. 11). The model does not take into account seasonal variable nutrient input from rivers driven by the monsoon system. The seasonality of external sources of nutrients is an important driver of chlorophyll-a variability at local scale.

Interannual variability

Figures 7, 8 and 9 present interannual anomalies of surface chlorophyll-a concentrations between 2008 and 2014 for model output and MODIS ocean colour averaged over three regions: South China Sea, Banda Sea and Sunda area. Simulated fields and satellite-derived chlorophyll-a are in good agreement in terms of amplitude and phasing, with temporal correlation coefficients of 0.56 for South China Sea and Banda sea and 0.87 for Sunda area. The model simulates a realistic temporal variability suggesting that processes regulating the seasonal as well as interannual variability of the Indonesian region are correctly reproduced. While the mean seasonal cycle of chlorophyll-a is driven by the strength and timing of the seasonal Asian monsoon, anomalies are driven by interannual climate modes, such as El Niño Southern Oscillation (ENSO) and Indian Ocean Dipole (IOD).

IOD drives the chlorophyll-a interannual variability in the eastern tropical Indian ocean, with a correlation coefficient of 0.74 (Fig. 9). IOD index and anomalies of chlorophyll-a from satellite give a similar correlation coefficient of 0.7. A positive phase of IOD indicates negative SST anomaly in the south-eastern tropical Indian Ocean associated with zonal wind anomaly along the equator (Meyers, 1996). The abnormally strong coastal upwelling near the Java Island stimulates a large phytoplankton bloom (Murtugudde et al., 1999). In the Banda

Sea and in South China Sea, no clear impact of ENSO or IOD is detected on the first level of the food chain (Fig. 7, 8). Inside the archipelago, both climate modes affect the variability of ITF transport, and it is not straightforward to separate their individual contribution (Masumoto, 2002; Sprintall and Révelard, 2014). Same comment can be done for the South China sea (Fig. 7).

While it is established (see references cited in Section 2) that ENSO and IOD climate modes play a key role in the Indonesian region, their impact on the marine ecosystem remains poorly understood. The length of simulation is too short for a rigorous assessment of the role of these drivers and a direct relationship is only evident in the Indian sector. However, interannual anomalies of simulated chlorophyll-a compare well to satellite observations, which suggests that interannual meteorological and ocean physical processes are satisfyingly reproduced by the model.

INDOMIX cruise

Model results are compared to INDOMIX in-situ data at three key locations: (1) the eastern entrance of Pacific waters to the archipelago (station 3, Halmahera Sea), (2) the convergence of the western and eastern pathways (station 4, Banda Sea) where intense tidal mixing and upwelling transforms Pacific waters to form the ITF, and (3) one of the main exit portals of the ITF to the Indian Ocean (station 5, Ombai Strait).

The vertical profile of temperature compares well to the data in the Halmahera Sea (Fig. 12). Simulated surface waters are too salty and the subsurface salinity maximum is reproduced at the observed depth, albeit underestimated compared to the data. Waters are more oxygenated in the model over the first 400 m. The model-data bias on temperature, salinity and oxygen suggests that Halmahera Sea thermocline waters are not correctly reproduced by the model in July 2010. The model tends to yield too smooth vertical profiles. Vertical profiles of nitrate and phosphate are well reproduced, while dissolved Si concentrations are overestimated below 200 m depth. It should be noted, however, that 2010 was a strong La Niña year with important modifications in zonal winds, rainfall, river discharges and ocean currents. While interannual variability is taken into account in atmospheric forcing and physical open boundary conditions, this is not the case for biogeochemistry. External inputs from rivers are constant, and open boundary conditions come from monthly climatologies. Dissolved Si profiles computed from the monthly WOA2009 climatology are close to simulated

distributions (not shown), suggesting non-standard conditions during the time of the INDOMIX cruise.

Despite the bias highlighted for Halmahera sea station, an overall satisfying correspondence between modelled and observed profiles is found at the Banda Sea (Fig. 13) and Ombai Strait stations (Fig. 14). The comparison of modelled profiles and cruise data along the flow path of waters from the Pacific to the Indian Ocean (from Halmahera to Ombai Strait) suggests that either the Halmahera Sea had no major influence for the ITF formation during the time of the cruise, or that vertical mixing and upwelling processes across the archipelago are strong enough to allow the formation of Indonesian water masses despite biases in source water composition. Alternatively, it could reflect the weak impact of ENSO on biogeochemical tracer distributions inside the archipelago compared to its Pacific border and the dominant role of Indian ocean dynamics on the ITF (Sprintall and Révelard, 2014).

Discussions and conclusions

The INDESO project aims to monitor and forecast marine ecosystem dynamics in Indonesian waters. A suit of numerical models has been coupled for setting up a regional configuration (INDO12) adapted to Indonesian seas. A forecasting oceanographic centre is fully operational in Perancak (Bali, Indonesia) since mid-September 2014. Here we access the skill of the OPA-NEMO hydrodynamical model coupled to the PISCES biogeochemical model (INDO12BIO configuration). A 8-year long hindcast simulation was launched in January 2007 and has caught up with real time. The strengths of the simulation are reminded below and weaknesses are discussed as follow: coastal ocean, cross-shore gradient and open ocean.

The large scale distribution of nutrient, oxygen, chlorophyll-*a*, NPP and mesozooplankton biomass are well reproduced. The vertical distribution of nutrient and oxygen is comparable to in-situ based datasets. Biogeochemical characteristics of North Pacific tropical waters entering in the archipelago are set by the open boundary. The transformation of water masses by hydrodynamics across the Indonesian archipelago is satisfyingly simulated. As a result, nitrate and oxygen vertical distributions match observations in Banda Sea and at the exit of the archipelago. The seasonal cycle of surface chlorophyll-*a* is in phase with satellite estimations. The northern and southern parts of the archipelago present a distinct seasonal cycle, with higher chlorophyll concentrations in the southern part during SE monsoon, and in the northern part of the archipelago during NW monsoon. The interannual variability of

surface chlorophyll-*a* correlates with satellite observations in several regions (South China sea, Banda sea and Indian part). These anomalies suggest that meteorological and ocean physical processes that drive the interannual variability in the Indonesian region are correctly reproduced by the model. The relative contribution of ENSO and IOD interannual climate modes to the interannual variability of chlorophyll-*a* is still an open question, and will be deepened in a future study.

Mean chlorophyll-*a* ($0.53 \text{ mg Chl m}^{-3}$) and NPP ($61 \text{ mmol C m}^{-2} \text{ d}^{-1}$) are systematically overestimated. Around the coasts, the temporal correlation between simulated chlorophyll-*a* and satellite data is breaks down. Simulated vertical profiles of nutrient and oxygen are diffusive as compared to data.

In coastal waters, chlorophyll-*a* concentrations are influenced by sedimentary processes (i.e. remineralization of organic carbon and subsequent release of nutrients) and riverine nutrient input. The slight disequilibrium introduced between the external input of nutrients and carbon and the loss to the sediment is sufficient to enhance chlorophyll-*a* concentrations along the coasts in line with observations. The sensitivity of the model to the balancing of carbon and nutrients at the lower boundary of the domain (“sediment burial”) highlights the need for an explicit representation of sedimentary reactions.

In order to further improve modelled chlorophyll-*a* variability along the coast, time-variant river nutrient and carbon fluxes will be needed. According to Jennerjahn et al. (2004), river discharges from Java can be increased by a factor of ~ 12 during NW monsoon as compared to SE monsoon. Moreover the maximum fresh water transport and the peak of material reaching the sea can be out of phase depending on the origin of discharged material (Hendiarti et al., 2004). The improved representation of river discharge dynamics and associated delivery of fresh water, nutrients and suspended matter in the model is, however, hampered by the availability of data. Most of the Indonesian rivers are currently not monitored (Susanto et al., 2006).

Systematic misfits between modelled and observed biogeochemical distributions may in part also reflect inherent properties of implemented numerical schemes. Misfits highlighted throughout this work include too much chlorophyll-*a*, and NPP on the shelves, with too weak cross-shore gradients between shelf and open waters, together with noticeable smoothing of vertical profiles of nutrients and oxygen. Currently, the MUSCL advection scheme is used for biogeochemical tracers. This scheme is too diffusive and smooths vertical profiles of

biogeochemical tracers. As a result, too much nutrients are injected in the surface layer and trigger high levels of chlorophyll-*a* and NPP. Another advection scheme, QUICKEST (Leonard, 1979) with the limiter of Zalezak (1979), already used in NEMO for the advection scheme of the physical model, has been tested for biogeochemical tracers. Switching from MUSCL to QUICKEST-Zalezak accentuates the vertical gradient of nutrients in the water column and attenuates modelled chlorophyll-*a* and NPP. This advection scheme is not diffusive and its use would be coherent with choices adopted for physical tracers. However, it results in an overestimation of the vertical gradient of nutrients, and the nutricline is considerably strengthened. Neither tuning of biogeochemical parameters, nor switching the advection scheme for passive tracers fully resolved the model-data misfits. Improving the vertical distribution of nutrients and oxygen, as well as chlorophyll-*a* and NPP in the open ocean and their cross-shore gradient relies at first order on the model physics.

Finally, monthly or yearly climatologies are currently used for initial and open boundary conditions. Biogeochemical tracers are thus decorrelated from model physics. In order to improve the link between modelled physics and biogeochemistry, weekly or monthly averaged output of the global ocean operational system operated by Mercator-Ocean (BIOMER) will be used in the future for the 24 tracers of the biogeochemical model PISCES. BIOMER will couple the physical forecasting system PSY3 to PISCES in off-line mode. The biogeochemical and the physical components of INDOBIO12 will thus be initialized and forced by the same PSY3 forecasting system.

Code and Data Availability

The INDO12 configuration is based on the NEMO 2.3 version developed by the NEMO consortium. All specificities included in the NEMO code version 2.3 are now freely available in the recent version NEMO 3.6 (<http://www.nemo-ocean.eu>). The biogeochemical model PISCES is coupled to hydrodynamic model by the TOP component of the NEMO system. PISCES 3.2 and its external forcing are also available via the NEMO web site. World Ocean Database and World ocean Atlas are available at <https://www.nodc.noaa.gov>. Glodap data are available at <http://cdiac.ornl.gov/oceans/glodap/GlopDV.html>. MODIS and MERIS ocean colour products are respectively available at <http://oceancolor.gsfc.nasa.gov/cms/> and <http://hermes.acri.fr/>, Primary production estimates based on VGPM, Eppley and CbPM algorithms at http://www.science.oregonstate.edu/ocean_productivity/.

Acknowledgements

The authors acknowledge financial support through the INDES0 (01/Balitbang KP.3/INDES0/11/2012) and Mercator-Vert (LEFE/GMMC) projects. They thank Christian Ethé for its technical advice on NEMO/PISCES. Ariane Koch-Larrouy provided INDOMIX data. We also thank our colleagues of Mercator Océan for their contribution to the model evaluation (Bruno Levier, Clément Bricaud, Julien Paul) and especially Eric Greiner for his useful recommendations and advice on the manuscript.

References

- Allen, G. R.: Conservation hotspots of biodiversity and endemism for Indo-Pacific coral reef fishes, *Aquatic Conserv: Mar. Freshw. Ecosyst.*, 18: 541–556, doi:10.1002/aqc.880, 2008.
- Allen, G. R., and Werner, T. B.: Coral Reef Fish Assessment in the ‘Coral Triangle’ of Southeastern Asia, *Environmental Biology of Fishes*, 65(2), 209–214, doi:10.1023/A:1020093012502, 2002.
- Alongi, D. A., da Silva, M., Wasson, R. J., and Wirasantosa, S.: Sediment discharge and export of fluvial carbon and nutrients into the Arafura and Timor Seas: A regional synthesis, *Marine Geology*, 343, 146–158, doi:10.1016/j.margeo.2013.07.004, 2013.
- Aumont, O., and Bopp, L.: Globalizing results from ocean in situ iron fertilization studies, *Global Biogeochem. Cycles*, 20, GB2017, doi:10.1029/2005GB002591, 2006.
- Aumont, O., Maier-Reimer, E., Blain, S., and Monfray, P.: An ecosystem model of the global ocean including Fe, Si, P colimitations. *Global Biogeochem. Cycles*, 17(2), 1060, doi:10.1029/2001GB001745, 2003.
- Ayers, J. M., Strutton, P. G., Coles, V. J., Hood, R. R., and Matear, R. J.: Indonesian throughflow nutrient fluxes and their potential impact on Indian Ocean productivity, *Geophys. Res. Lett.*, 41(14), 5060–5067, doi:10.1002/2014GL060593, 2014.
- Behrenfeld, M. J., and Falkowski, P. G.: Photosynthetic rates derived from satellite-based chlorophyll concentration, *Limnol. Oceanogr.*, 42(1), 1–20, 1997.
- Behrenfeld, M. J., Boss, E., Siegel, D. A., and Shea, D. M.: Carbon-based ocean productivity and phytoplankton physiology from space, *Global Biogeochem. Cycles*, 19(1), GB1006, doi:10.1029/2004GB002299, 2005.
- Bryant, D., Burke, L., McManus, J., and Spalding, M.: *Reefs at Risk: A Map-Based Indicator of Potential Threats to the World’s Coral Reefs*, World Resources Institute, Washington, DC; International Center for Living Aquatic Resource Management, Manila; and United Nations Environment Programme–World Conservation Monitoring Centre, Cambridge, 1998.
- Buitenhuis, E. T., Vogt, M., Moriarty, R., Bednaršek, N., Doney, S. C., Leblanc, K., Le Quéré, C., Luo, Y.-W., O'Brien, C., O'Brien, T., Peloquin, J., Schiebel, R., and Swan, C.: MAREDAT: towards a world atlas of MARine Ecosystem DATA, *Earth Syst. Sci. Data*, 5, 227–239, doi:10.5194/essd-5-227-2013, 2013.

Cros, A., Fatan, N. A. White, A., Teoh S. J., Tan, S., Handayani, C., Huang, C., Peterson, N., Li, R. V., Siry, H. Y., Fitriana, R., Gove, J., Acoba, T., Knight, M., Acosta, R., Andrew, N., and Beare, D.: The Coral Triangle Atlas: An Integrated Online Spatial Database System for Improving Coral Reef Management, *PLoS ONE* 9(6): e96332. doi:10.1371/journal.pone.0096332, 2014.

CSIRO: Atlas of Regional Seas, available at: <http://www.marine.csiro.au/~dunn/cars2009/> (last access: 13 August 2015), 2009.

Doerffer, R. and Schiller, H: The MERIS Case 2 water algorithm, *International Journal of Remote Sensing*, 28, 517-535, doi:10.1080/01431160600821127, 2007.

FAO: United Nations Food and Agricultural Organization, FAOSTAT, available at: <http://faostat.fao.org/site/291/default.aspx> (last access: 13 August 2015), 2007.

Ffield, A., and Gordon, A. L.: Vertical Mixing in the Indonesian Thermocline, *J. Phys. Oceanogr.*, 22, 184-195, 1992.

Ffield, A., and Gordon, A. L.: Tidal mixing signatures in the Indonesian Seas. *J. Phys. Oceanogr.*, 26, 1924–1937, 1996.

Foale, S., Adhuri, D., Aliño, P., Allison, E. H., Andrew, N., Cohen, P., Evans, L., Fabinyi, M., Fidelman, P., Gregory, C., Stacey, N., Tanzer, J., and Weeratunge, N.: Food security and the Coral Triangle Initiative, *Marine Policy*, 38, 174-183, doi:10.1016/j.marpol.2012.05.033, 2013.

Garcia, H. E., Locarnini, R. A., Boyer, T. P., Antonov, J. I., Baranova, O. K., Zweng, M. M., and Johnson, D. R.: World Ocean Atlas 2009, Volume 3: Dissolved Oxygen, Apparent Oxygen Utilization, and Oxygen Saturation. S. Levitus, Ed. NOAA Atlas NESDIS 70, U.S. Government Printing Office, Washington, D.C., 344 pp., 2010a.

Garcia, H. E., Locarnini, R. A., Boyer, T. P., Antonov, J. I., Zweng, M. M., Baranova, O. K., and Johnson, D. R.: World Ocean Atlas 2009, Volume 4: Nutrients (phosphate, nitrate, silicate). S. Levitus, Ed. NOAA Atlas NESDIS 71, U.S. Government Printing Office, Washington, D.C., 398 pp., 2010b.

Ginsburg, R. N.: Ed., Proceedings of the Colloquium on Global Aspects of Coral Reefs: Health, Hazards and History, Atlantic Reef Committee, 1994.

Gordon, A. L: Oceanography of the Indonesian seas and their throughflow, *Oceanography*, 18(4), 14–27, doi:10.5670/oceanog.2005.01, 2005.

Green, A., and Mous, P. J.: Delineating the Coral Triangle, its ecoregions and functional seascapes. Report on an expert workshop held in Southeast Asia Center for Marine Protected Areas, Bali, Indonesia, April 30-May 2, 2003, The Nature Conservancy, 2004.

Hendiarti, N., Siegel, H., and Ohde, T.: Investigation of different coastal processes in Indonesian waters using SeaWiFS data, *Deep-Sea Research Part II*, 51(1-3), 85-97, doi:10.1016/j.dsr2.2003.10.003, 2004.

Hendiarti, N., Suwarso, E., Aldrian, E., Amri, K., Andiastruti, R., Sachoemar, S. I., and Wahyono, I. B.: Seasonal variation of pelagic fish catch around Java, *Oceanography*, 18(4), 112-123, doi:10.5670/oceanog.2005.12, 2005.

Henson, S. A., Sarmiento, J. L., Dunne, J. P., Bopp, L., Lima, I., Doney, S. C., John, J., and Beaulieu, C.: Detection of anthropogenic climate change in satellite records of ocean chlorophyll and productivity, *Biogeosciences*, 7(2), 621–640, doi:10.5194/bg-7-621-2010, 2010.

Hirst, A. C., and Godfrey, J. S.: The role of Indonesian ThroughFlow in a global ocean GCM, *J. Phys. Oceanogr.*, 23(6), 1057–1086, 1993.

Hopley, D. and Suharsono, M.: *The Status of Coral Reefs in Eastern Indonesia*. Australian Institute of Marine Science, Townsville, Australia, 2000.

Jennerjahn, T. C., Ittekkot, V., Klopper, S., Adi, S., Purwo Nugroho, S., Sudiana, N., Yusmal, A., and Gaye-Haake, B.: Biogeochemistry of a tropical river affected by human activities in its catchment: Brantas River estuary and coastal waters of Madura Strait, Java, Indonesia, *Estuarine Coastal Shelf Sci.*, 60(3), 503–514, doi:10.1016/j.ecss.2004.02.008, 2004.

Key, R. M., Kozyr, A., Sabine, C. L., Lee, K., Wanninkhof, R., Bullister, J., Feely, R.A., Millero, F., Mordy, C. and Peng, T.-H.: A global ocean carbon climatology: Results from GLODAP. *Global Biogeochemical Cycles*, Vol. 18, GB4031, 2004.

Koch-Larrouy, A., Madec, G., Bouruet-Aubertot, P., Gerkema, T., Bessieres, L., and Molcard, R.: On the transformation of Pacific Water into Indonesian Throughflow Water by internal tidal mixing, *Geophys. Res. Lett.*, 34, L04604, doi:10.1029/2006GL028405, 2007.

Koch-Larrouy, A., Morrow, R., Penduff, T., and Juza, M.: Origin and mechanism of Subantarctic Mode Water formation and transformation in the Southern Indian Ocean, *Ocean Dynamics*, 60(3), 563-583, doi:10.1007/s10236-010-0276-4, 2010.

Koch-Larrouy, A., Atmadipoera, A., Van Beek, P., Madec, G., Aucan, J., Lyard, F., Grelet, J.

and Souhaut, M.: Estimates of tidal mixing in the Indonesian archipelago from multidisciplinary INDOMIX in-situ data, Deep Sea Research part 1, M DSR1-D-14-00245R1, in revision, 2015.

Lehodey, P., Senina, I., and Murtugudde, R.: A spatial ecosystem and populations dynamics model (SEAPODYM) – Modeling of tuna and tuna-like populations, *Progress in Oceanography*, 78, 304–318, 2008.

Leonard, B. P.: A stable and accurate convective modelling procedure based on quadratic upstream interpolation, *Comp. Method. Appl. M.* 19, 59–98, 1979.

Lévy, M., Estublier, A., and Madec, G.: Choice of an Advection Scheme for Biogeochemical Models, *Geophysical Research Letters*, 28(19), 3725-3728, 2001.

Ludwig, W., Probst, J. L., and Kempe, S.: Predicting the oceanic input of organic carbon by continental erosion, *Global Biogeochem.Cycles*, 10(1), 23– 41, doi:10.1029/95GB02925, 1996.

Madden, R. A., and Julian P. R.: Observations of the 40–50 day tropical oscillation - A review, *Monthly Weather Reviews*, 122(5), 814–837, 1994.

Madec G.: "NEMO ocean engine", Note du Pole de modélisation, Institut Pierre-Simon Laplace (IPSL), France, No 27 ISSN No 1288-1619, 2008.

Madec, G., Delecluse, P., Imbard, M., and Lévy, C.: "OPA 8.1 Ocean General Circulation Model reference manual", Note du Pole de modélisation, Institut Pierre-Simon Laplace (IPSL), France, No11, 91pp., 1998.

Masumoto, Y.: Effects of Interannual Variability in the Eastern Indian Ocean on the Indonesian Throughflow, *Journal of Oceanography*, 58, 175-182, 2002.

Meyers, G.: Variation of Indonesian throughflow and the El Niño-Southern Oscillation. *J. Geophys. Res.*, 101, 12,475–12,482, 1996.

Milliman, J. D., Farnsworth, K. L., and Albertin, C. S.: Flux and fate of fluvial sediments leaving large islands in the East Indies, *J. Sea Res.*, 41(1-2), 97–107, 1999.

Moore, T. S., Campbell, J. W., and Dowell, M. D: A class-based approach to characterizing and mapping the uncertainty of the MODIS ocean chlorophyll product, *Remote Sensing of Environment*, 113, 2424-2430, 2009.

Mora, C., Chittaro, P. M., Sale, P. F., Kritzer, J. P., and Ludsin, S.A.: Patterns and processes in reef fish diversity, *Nature*, 421, 933-936, doi:10.1038/nature01393, 2003.

Moriarty, R., and O'Brien, T. D.: Distribution of mesozooplankton biomass in the global ocean, *Earth System Science Data*, 5,45-55, 2013.

Murtugudde, R., Busalacchi, A. J., and Beauchamp, J.: Seasonal-to-interannual effects of the Indonesian Throughflow on the tropical Indo-Pacific Basin. *J. Geophys. Res.*, 103, 21,425–21,441, 1998.

Murtugudde, R., Signorini, S. R., Christian, J. R., Busalacchi, A. J., McClain, C. R., and Picaut, J.: Ocean color variability of the tropical Indo-Pacific basin observed by SeaWiFS during 1997–1998. *J. Geophys. Res.*, 104, 18,351–18,366, 1999.

Pimentel D., Harvey, C., Resosudarmo, P., Sinclair, K., Kurz, D., McNair, M., Crist, C., Shpritz, L., Fitton, L., Saffouri, R., and Blair, R.: Environmental and Economic Costs of Soil Erosion and Conservation Benefits, *Science*, 267(5201), 1117-1123, 1995.

Potemra, J. T., Lukas, R., and Mitchum, G. T.: Large-scale estimation of transport from the Pacific to the Indian Ocean. *J. Geophys. Res.*, 102, 27,795–27,812, 1997.

Rixen, T., Ittekkot, V., Herunadi, B., Wetzel, P., Maier-Reimer, E., and Gaye-Haake, B.: ENSO-driven carbon see saw in the Indo-Pacific, *Geophys. Res. Lett.*, 33, L07606, doi:10.1029/2005GL024965, 2006.

Roberts, C. M., McClean, C. J., Veron, J. E. N., Hawkins, J. P., Allen, G. R., McAllister, D. E., Mittermeier, C. G., Schueler, F. W., Spalding, M., Wells, F., Vynne, C., and Werner, T. B.: Marine Biodiversity Hotspots and Conservation Priorities for Tropical Reefs, *Science*, 295(5558), 1280-1284, doi:10.1126/science.1067728, 2002.

Romero, O. E., Rixen, T., and Herunadi, B.: Effects of hydrographic and climatic forcing on diatom production and export in the tropical southeastern Indian Ocean, *Mar. Ecol. Prog. Ser.*, 384, 69-82, doi:10.3354/meps08013, 2009.

Saji, N. H., Goswami, B. N., Vinayachandran, P. N., and Yamagata, T.: A dipole mode in the tropical Indian Ocean. *Nature*, 401, 360–363, 1999.

Sprintall, J., Gordon, A. L., Murtugudde, R., and Susanto, R. D.: A semi-annual Indian Ocean forced Kelvin waves observed in the Indonesian Seas, May 1997. *J. Geophys. Res.*, 105(C7), 17217–17230, doi:10.1029/2000JC900065, 2000.

- Sprintall, J., and Révelard, A.: The Indonesian throughflow response to Indo-Pacific climate variability, *J. Geophys. Res. Oceans*, 119, 1161–1175, doi:10.1002/2013JC009533, 2014.
- Susanto, R. D., and Marra, J.: Effect of the 1997/98 El Niño on chlorophyll a variability along the southern coasts of Java and Sumatra, *Oceanography*, 18(4), 124–127, doi:10.5670/oceanog.2005.13, 2005.
- Susanto, R. D., Gordon, A. L., Sprintall, J., and Herunadi, B.: Intraseasonal variability and tides in Makassar Strait. *Geophys. Res. Lett.*, 27, 1499–1502, 2000.
- Susanto, R. D., Gordon, A. L., and Zheng, Q.: Upwelling along the coasts of Java and Sumatra and its relation to ENSO, *Geophys. Res. Lett.*, 28(8), 1599–1602, doi:10.1029/2000GL011844, 2001.
- Susanto, R. D., Moore, T. S., and Marra, J.: Ocean color variability in the Indonesian Seas during the SeaWiFS era, *Geochemistry Geophysics Geosystems*, 7(5), Q05021, doi:10.1029/2005GC001009, 2006.
- Tegen, I., and Fung, I.: Contribution to the Atmospheric Mineral Aerosol Load From Land-Surface Modification, *J Geophys Res-Atmos*, 100, 18707–18726, 1995.
- Tranchant, B., Reffray, G., Greiner, E., Nugroho, D., Koch-Larrouy, A., and Gaspar, P.: Evaluation of an operational ocean model configuration at 1/12° spatial resolution for the Indonesian seas. Part I: ocean physics, *Geosci. Model Dev. Discuss.*, 8, 6611–6668, doi:10.5194/gmdd-8-6611-2015, 2015.
- UNEP: Vantier, L., Wilkinson, C., Lawrence, D. and Souter, D. (Eds.): Indonesian Seas, GIWA Regional Assessment 57, University of Kalmar, Kalmar, Sweden, 2005.
- UNEP: Sherman, K. and Hempel, G. (Eds.): The UNEP Large Marine Ecosystem Report: A perspective on changing conditions in LMEs of the world's Regional Seas, United Nations Environment Programme. Nairobi, Kenya, 2009.
- Van Leer, B.: Towards the Ultimate Conservative Difference Scheme. IV. A New Approach to Numerical Convection, *J. Comput. Phys.*, 23, 276–299, 1977.
- Veron, J. E. E., Devantier, L. M., Turak, E., Green, A. L., Kininmonth, S., Stafford-Smith, M., and Peterson, N.: Delineating the Coral Triangle, *Galaxea, J. Coral Reef Studies* 11, 91–100, 2009.

Westberry, T., Behrenfeld, M. J., Siegel, D. A., and Boss, E.: Carbon-based primary productivity modeling with vertically resolved photoacclimation, *Global Biogeochem. Cycles*, 22(2), GB2024, doi:10.1029/2007GB003078, 2008.

WOA: World Ocean Atlas, available at: http://www.nodc.noaa.gov/OC5/WOA09/pr_woa09.html (last access: 13 August 2015), 2009.

WOD: World Ocean Database, available at: http://www.nodc.noaa.gov/OC5/WOD09/pr_wod09.html (last access: 13 August 2015), 2009.

Wolter, K., and Timlin, M. S.: Measuring the strength of ENSO events - how does 1997/98 rank? *Weather*, 53, 315-324, 1998.

Wolter, K., and Timlin, M. S.: El Niño/Southern Oscillation behaviour since 1871 as diagnosed in an extended multivariate ENSO index (MEI.ext). *Intl. J. Climatology*, 31, 1074-1087, 2011.

Zalezak, S. T.: Fully multidimensional flux-corrected transport algorithms for fluids, *J. Computat. Phys.*, 31, 335-362, 1979.

Table caption

Table 1. Initial and open boundary conditions used for the INDO12BIO configuration.

Figure caption

Figure 1. Temporal evolution of total carbon (a), plankton (b), DIC and DOC (c) and nutrient (d, e) content averaged over the whole 3-dimensional INDO12BIO domain.

Figure 2: Annual mean of nitrate (mmol N m^{-3} ; left) and oxygen concentrations ($\text{ml O}_2 \text{ l}^{-1}$; right) at 100 m depth from CARS (a, d) and WOA (b, e; statistical mean) annual climatologies, and from INDO12BIO as 2010-2014 averages (c, f). Three key boxes for water mass transformation (North Pacific, Banda, and Timor; Koch-Larrouy et al., 2007) were added to the bottom-right figure.

Figure 3: Vertical profiles of oxygen ($\text{ml O}_2 \text{ l}^{-1}$; top: a, d, g), nitrate (mmol N m^{-3} ; middle: b, e, h) and dissolved silica (mmol Si m^{-3} ; bottom: c, f, i) in 3 key boxes for water masses transformation (North Pacific, left; Banda, middle; and Timor, right) (see Fig. 2; Koch-Larrouy et al., 2007). CARS and WOA annual climatologies are in red and dark blue. INDO12BIO simulation averaged between 2010 and 2014 is in black. All the raw data available on each box and gathered in the WOD (light blue crosses) are added in order to illustrate the spread of data.

Figure 4. Left) Annual mean of surface chlorophyll-*a* concentrations (mg Chl m^{-3}) for year 2011: MODIS Case-1 product (a), MERIS Case-2 product (b) and INDO12BIO simulation (c). Right) Bias of log-transformed surface chlorophyll (model-observation) for the same year. The model was masked as a function of the observation, MODIS Case-1 (d) or MERIS Case-2 (e). Location of 3 stations sampled during the INDOMIX cruise and used for evaluation of the model in Section 4.4 (f).

Figure 5. Annual mean of vertically integrated primary production ($\text{mmol C m}^{-2} \text{ d}^{-1}$) for year 2011: VGPM (a), Eppley (d), and CbPM (b) production models, all based on MODIS ocean colour, as well as for INDO12BIO (e). Standard deviation of the 3 averaged production models (PM) (c), and bias between INDO12BIO and the average of PM (f).

Figure 6: Annual mean of mesozooplankton biomass ($\mu\text{g C l}^{-1}$) from MAREDAT monthly climatology (left) and from INDO12BIO simulation averaged between 2010 and 2014 (right), for distinct depth interval: from the surface up to 40m (a, e), 100m (b, f), 150m (c, g), and 200m depth (d, h). Simulated fields were interpolated onto the MAREDAT grid, and masked as a function of the data (in space and time).

Figure 7: a) Mean surface chlorophyll-*a* concentrations and b) its interannual anomalies (mg Chl m^{-3}) over the South China Sea. INDO12BIO is in black and MODIS Case-1 in red. Temporal correlation (*r*) between both time series is in black. c) ENSO (blue) and IOD (green) phenomena are respectively represented by MEI and DMI indexes. Indexes were normalized by their maximum value in order to be plotted on the same axis. Interannual anomalies of simulated chlorophyll-*a* are reminded in black. Temporal correlation (*r*) between the simulated chlorophyll-*a* and ENSO (IOD) is indicated in blue (green).

Figure 8: Same as Figure 7, in Banda Sea.

Figure 9: Same as Figure 7, in Sunda area.

Figure 10. Timing of maximum chlorophyll-*a* (a, c) and amplitude (b, d) for a monthly climatology of surface chlorophyll-*a* concentrations between 2010 and 2014: MODIS Case-1 (left) and INDO12BIO (right). The model was masked as a function of the data.

Figure 11: Temporal correlation (a) and normalised standard deviation (b; $\text{std}(\text{model})/\text{std}(\text{data})$) estimated between the INDO12BIO simulation and the MODIS Case-1 ocean colour product. Statistics are computed on monthly fields between 2010 and 2014. The model was masked as a function of the data.

Figure 12: Vertical profiles of temperature ($^{\circ}\text{C}$; a), salinity (psu; b), oxygen ($\text{ml O}_2 \text{l}^{-1}$; c), nitrate (mmol N m^{-3} ; d), phosphate (mmol P m^{-3} ; e), and dissolved silica (mmol Si m^{-3} ; f) concentrations at INDOMIX cruise Station 3 (Halmahera Sea; 13 - 14 July 2010). CTD (light blue lines) and bottle (red crosses) measurements represent the conditions during cruise, 2-day model averages are shown by the black line.

Figure 13: Vertical profiles of temperature ($^{\circ}\text{C}$; a), salinity (psu; b), oxygen ($\text{ml O}_2 \text{l}^{-1}$; c), nitrate (mmol N m^{-3} ; d), phosphate (mmol P m^{-3} ; e), and dissolved silica (mmol Si m^{-3} ; f) concentrations at INDOMIX cruise Station 4 (Banda Sea; 15 - 16 July 2010). CTD (light blue lines) and bottle (red crosses) measurements represent the conditions during cruise, 2-day model averages are shown by the black line.

Figure 14: Vertical profiles of temperature ($^{\circ}\text{C}$; a), salinity (psu; b), oxygen ($\text{ml O}_2 \text{ l}^{-1}$; c), nitrate (mmol N m^{-3} ; d), phosphate (mmol P m^{-3} ; e), and dissolved silica (mmol Si m^{-3} ; f) concentrations at INDOMIX cruise Station 5 (Ombai Strait; 16 - 17 July 2010). CTD (light blue lines) and bottle (red crosses) measurements represent the conditions during cruise, 2-day model averages are shown by the black line.

Table 1. Initial and open boundary conditions used for the INDO12BIO configuration.

Variables	Initial Conditions	OBC
NO₃, O₂, PO₄, Si	From WOA January ^a	WOA monthly ^a
DIC, ALK	GLODAP annual ^b	GLODAP annual ^b
DCHL, NCHL, PHY2, PHY1	From SeaWiFS January ^c	From SeaWiFS monthly ^c
NH₄	Analytical profile ^d	Analytical profile ^d
DOC, Fe	ORCA2 January	ORCA2 monthly

^a: From World Ocean Atlas (WOA 2009) monthly climatology, with increased nutrient concentrations along the coasts (necessary adaptation due to crucial lack of data in the studied area).

^b: Key et al. (2004).

^c: From SeaWiFS monthly climatology. Phytoplankton is deduced using constant ratios of 1.59 g Chl mol N⁻¹ and 122/16 mol C mol N⁻¹, and exponential decrease with depth.

^d: Low values offshore and increasing concentrations onshore.

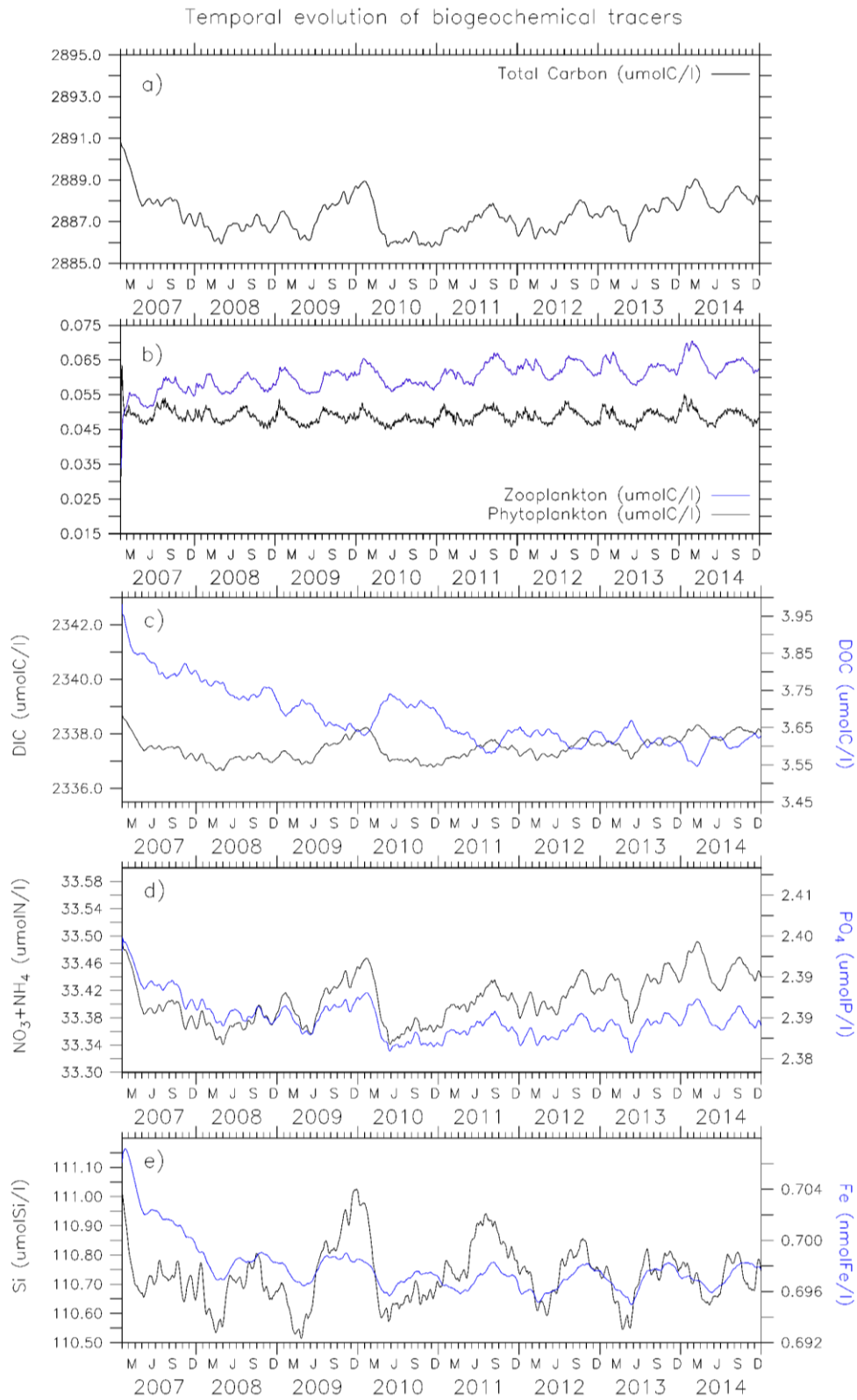


Figure 1. Temporal evolution of total carbon (a), plankton (b), DIC and DOC (c) and nutrient (d, e) content averaged over the whole 3-dimensional INDO12BIO domain.

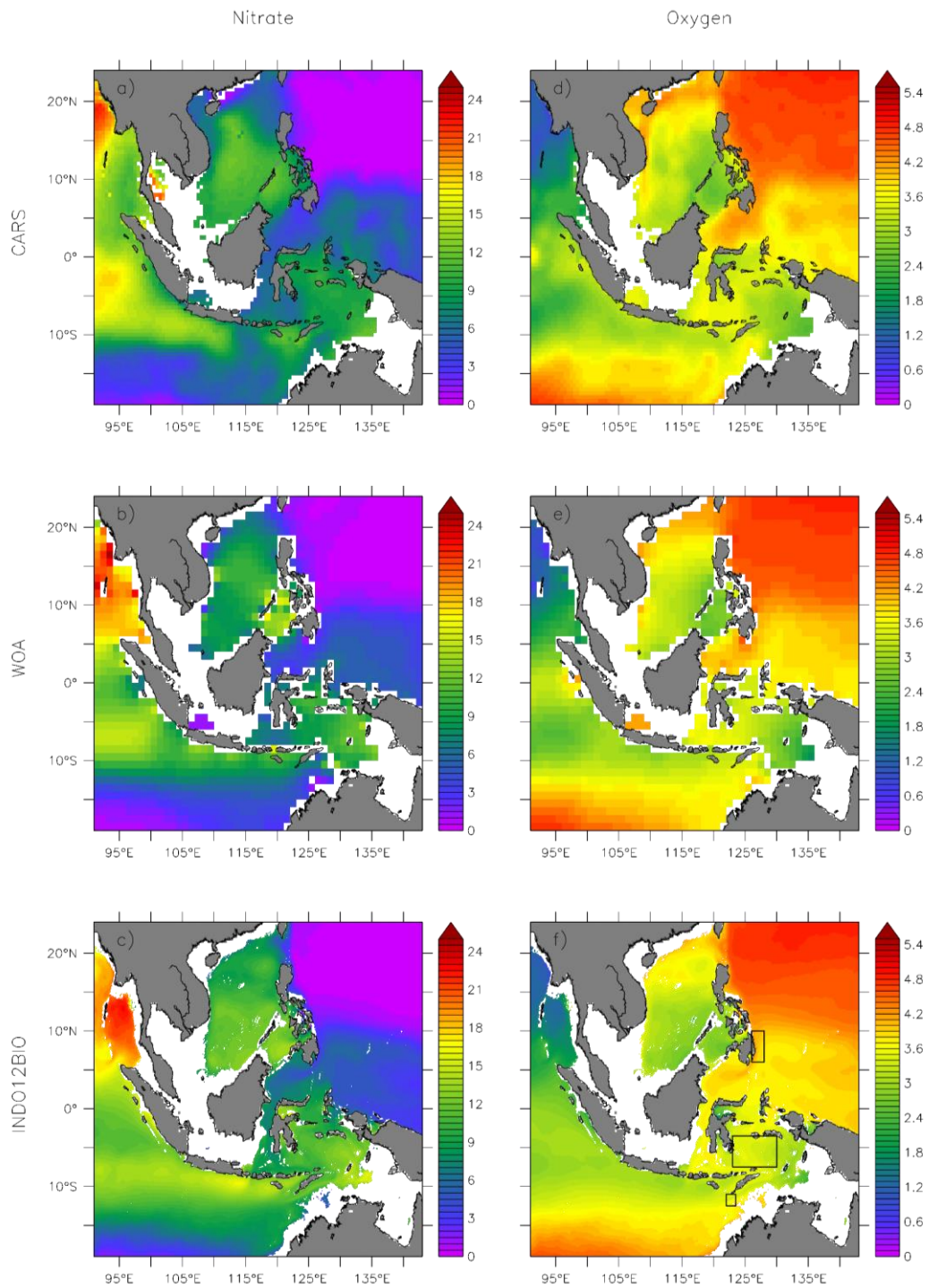


Figure 2: Annual mean of nitrate (mmol N m^{-3} ; left) and oxygen concentrations ($\text{ml O}_2 \text{l}^{-1}$; right) at 100 m depth from CARS (a, d) and WOA (b, e; statistical mean) annual climatologies, and from INDO12BIO as 2010-2014 averages (c, f). Three key boxes for water mass transformation (North Pacific, Banda, and Timor; Koch-Larrouy et al., 2007) were added to the bottom-right figure.

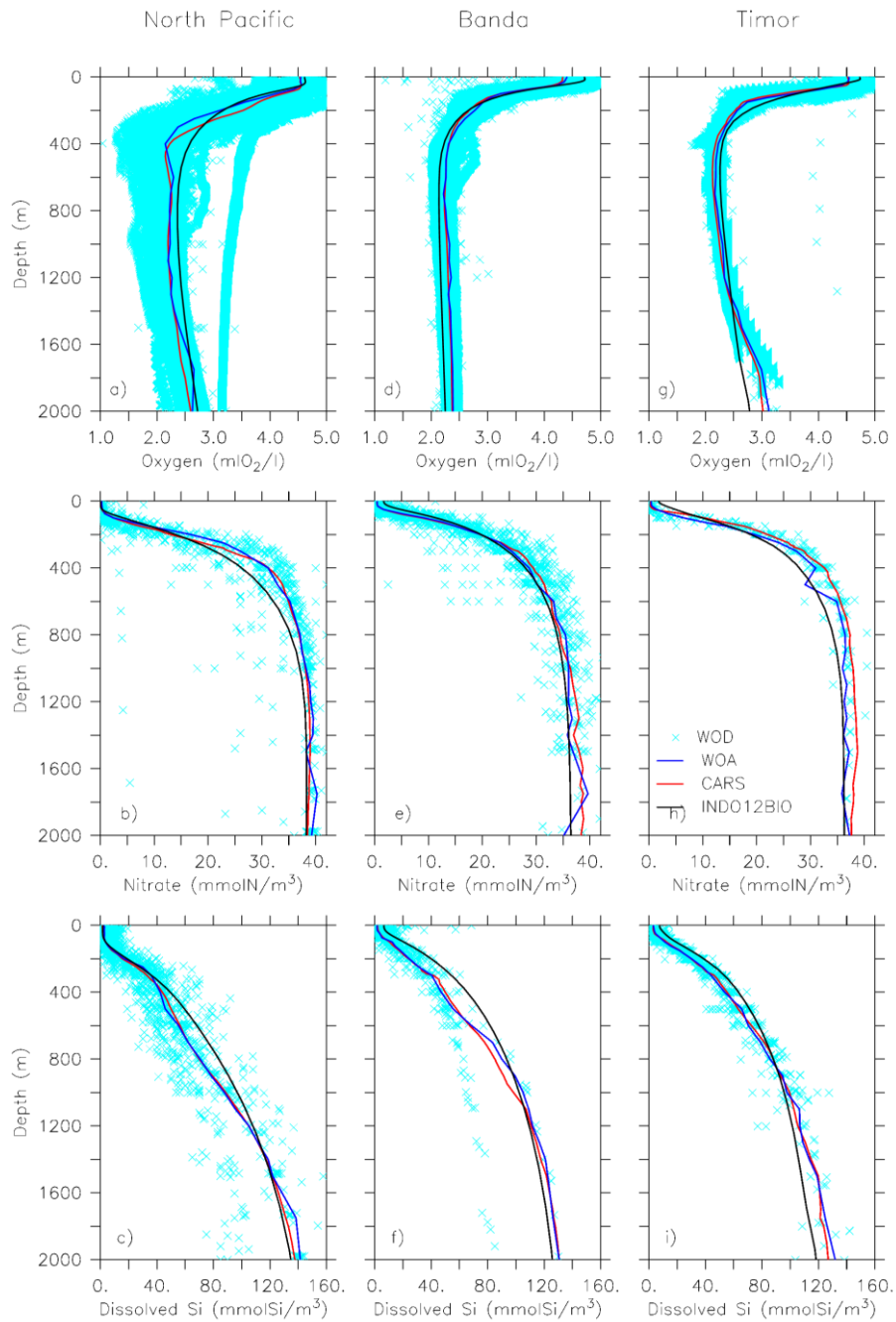


Figure 3: Vertical profiles of oxygen ($\text{ml O}_2 \text{ l}^{-1}$; top: a, d, g), nitrate (mmol N m^{-3} ; middle: b, e, h) and dissolved silica (mmol Si m^{-3} ; bottom: c, f, i) in 3 key boxes for water masses transformation (North Pacific, left; Banda, middle; and Timor, right) (see Fig. 2; Koch-Larrouy et al., 2007). CARS and WOA annual climatologies are in red and dark blue. INDO12BIO simulation averaged between 2010 and 2014 is in black. All the raw data available on each box and gathered in the WOD (light blue crosses) are added in order to illustrate the spread of data.

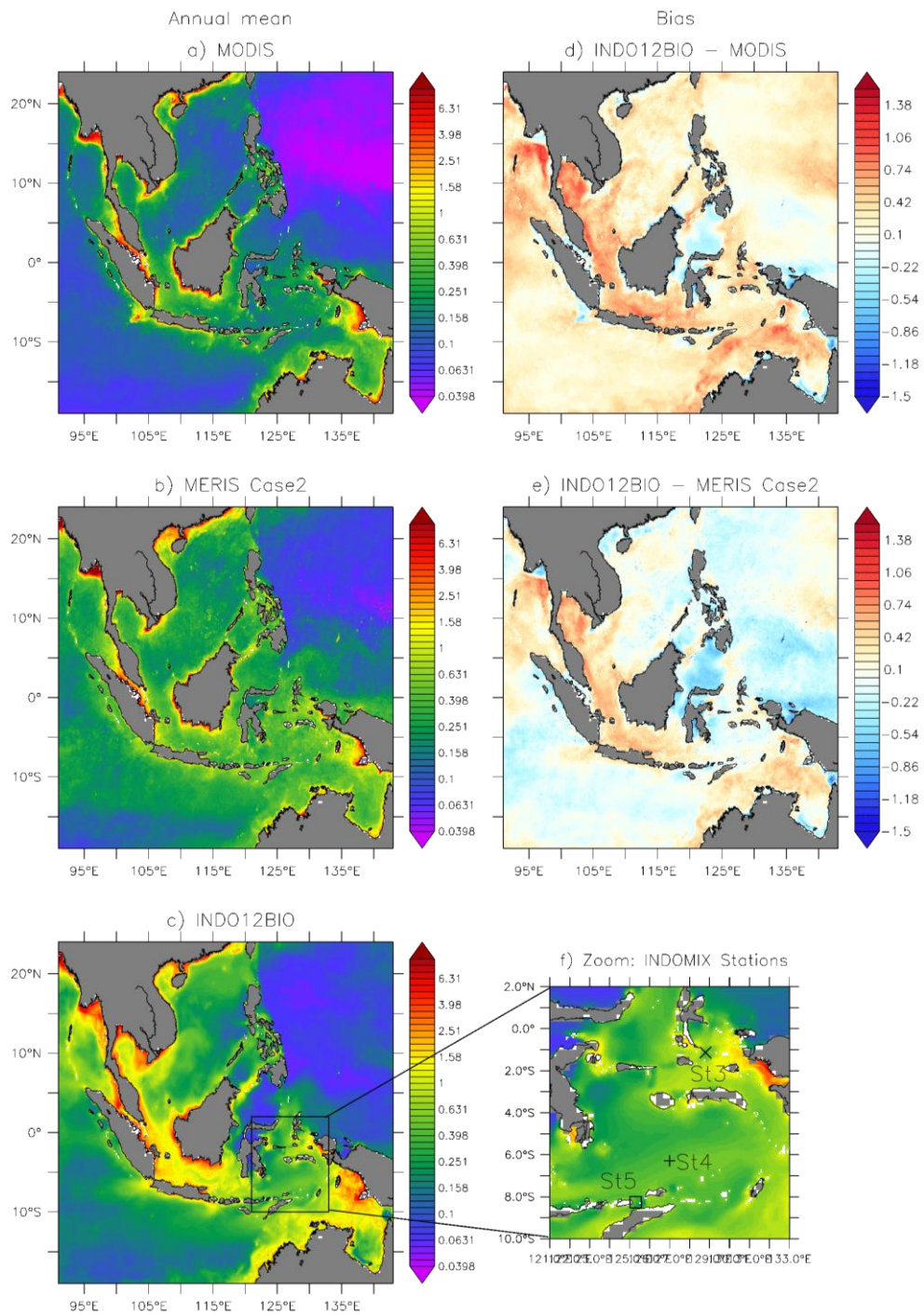


Figure 4. Left) Annual mean of surface chlorophyll-*a* concentrations (mg Chl m^{-3}) for year 2011: MODIS Case-1 product (a), MERIS Case-2 product (b) and INDO12BIO simulation (c). Right) Bias of log-transformed surface chlorophyll (model-observation) for the same year. The model was masked as a function of the observation, MODIS Case-1 (d) or MERIS Case-2 (e). Location of 3 stations sampled during the INDOMIX cruise and used for evaluation of the model in Section 4.4 (f).

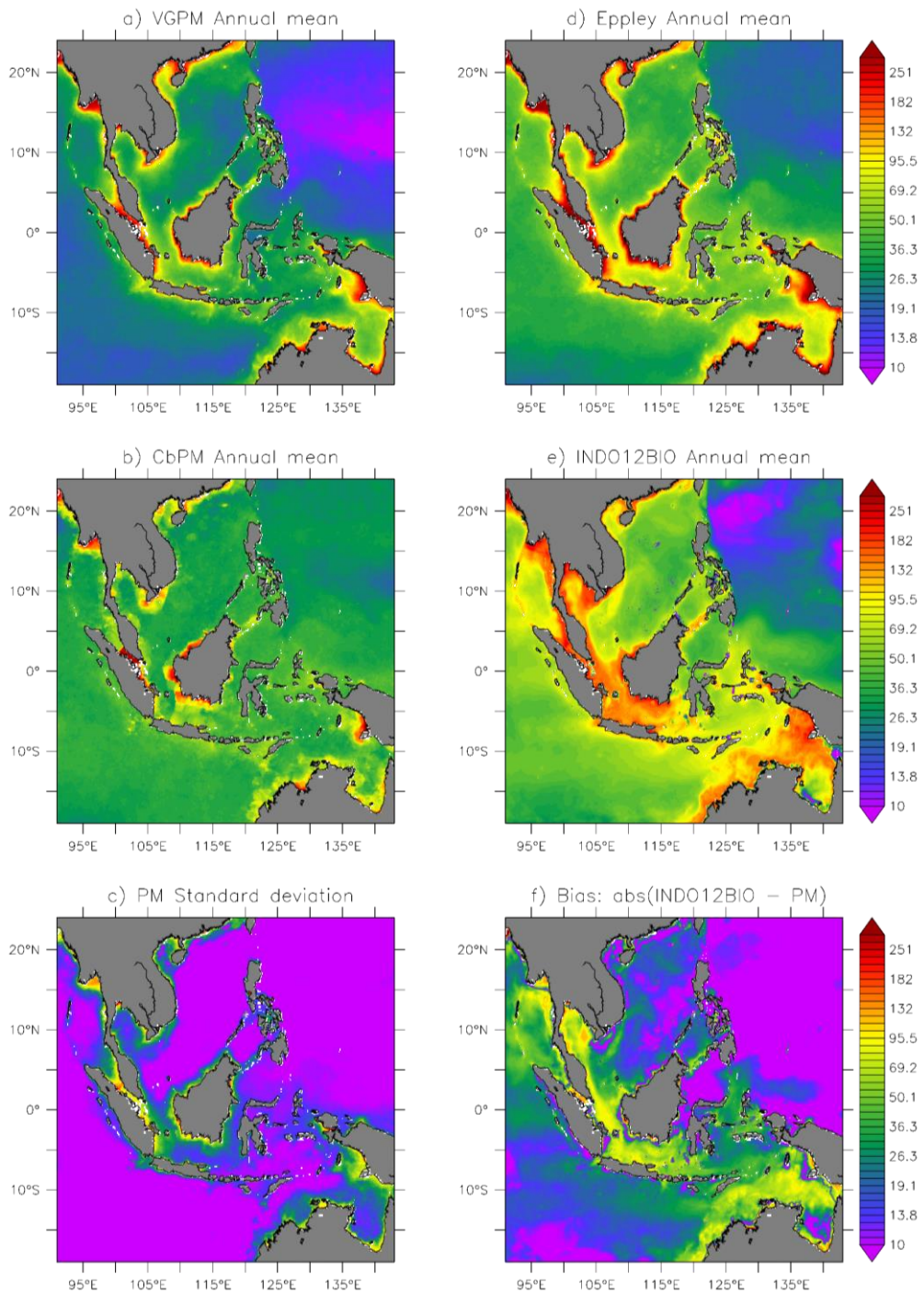


Figure 5. Annual mean of vertically integrated primary production ($\text{mmol C m}^{-2} \text{d}^{-1}$) for year 2011: VGPM (a), Eppley (d), and CbPM (b) production models, all based on MODIS ocean colour, as well as for INDO12BIO (e). **Standard deviation of the 3 averaged production models (PM)** (c), and bias between INDO12BIO and the averaged PM (f).

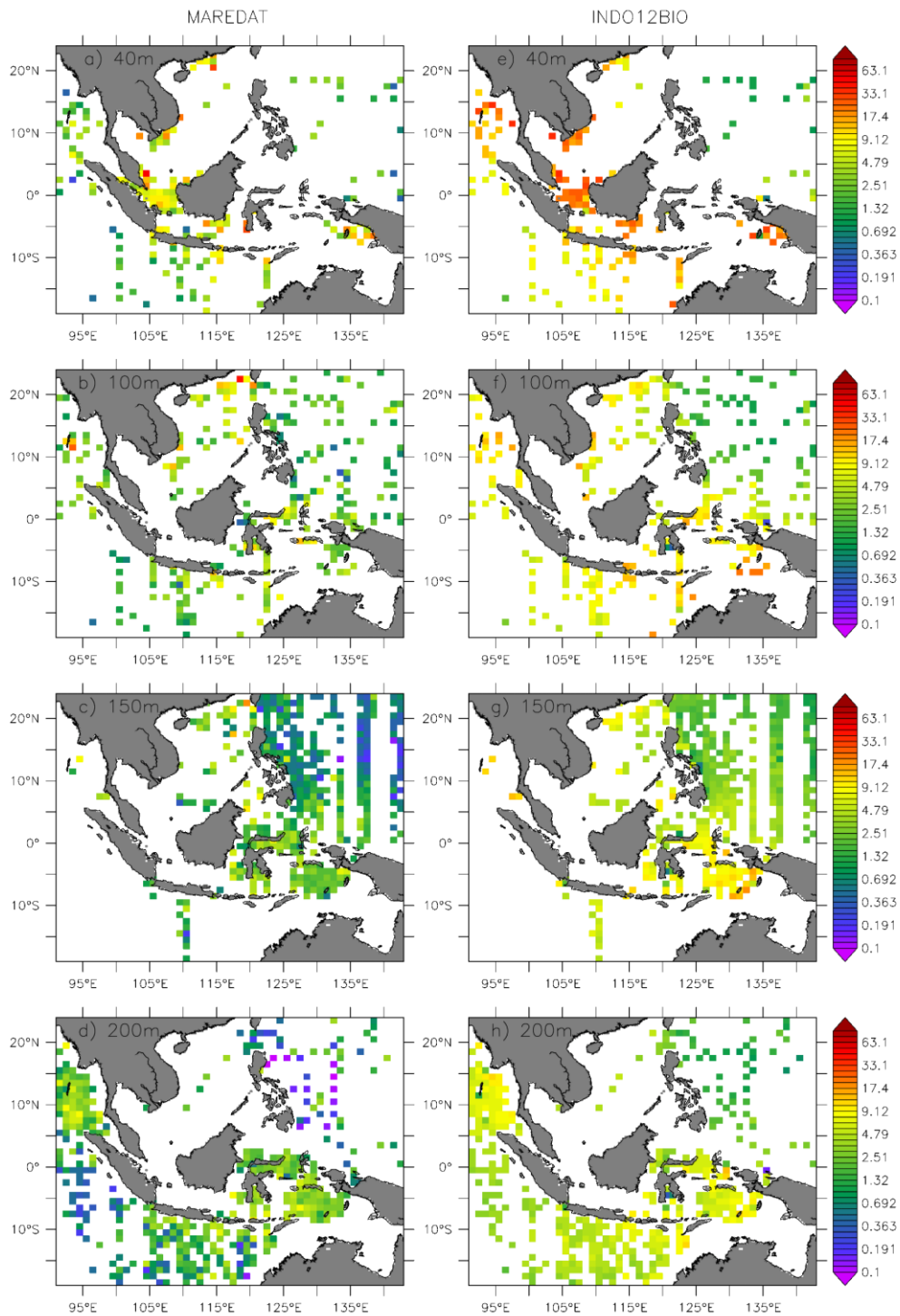


Figure 6: Annual mean of mesozooplankton biomass ($\mu\text{g C l}^{-1}$) from MAREDAT monthly climatology (left) and from INDO12BIO simulation averaged between 2010 and 2014 (right), for distinct depth interval: from the surface up to 40m (a, e), 100m (b, f), 150m (c, g), and 200m depth (d, h). Simulated fields were interpolated onto the MAREDAT grid, and masked as a function of the data (in space and time).

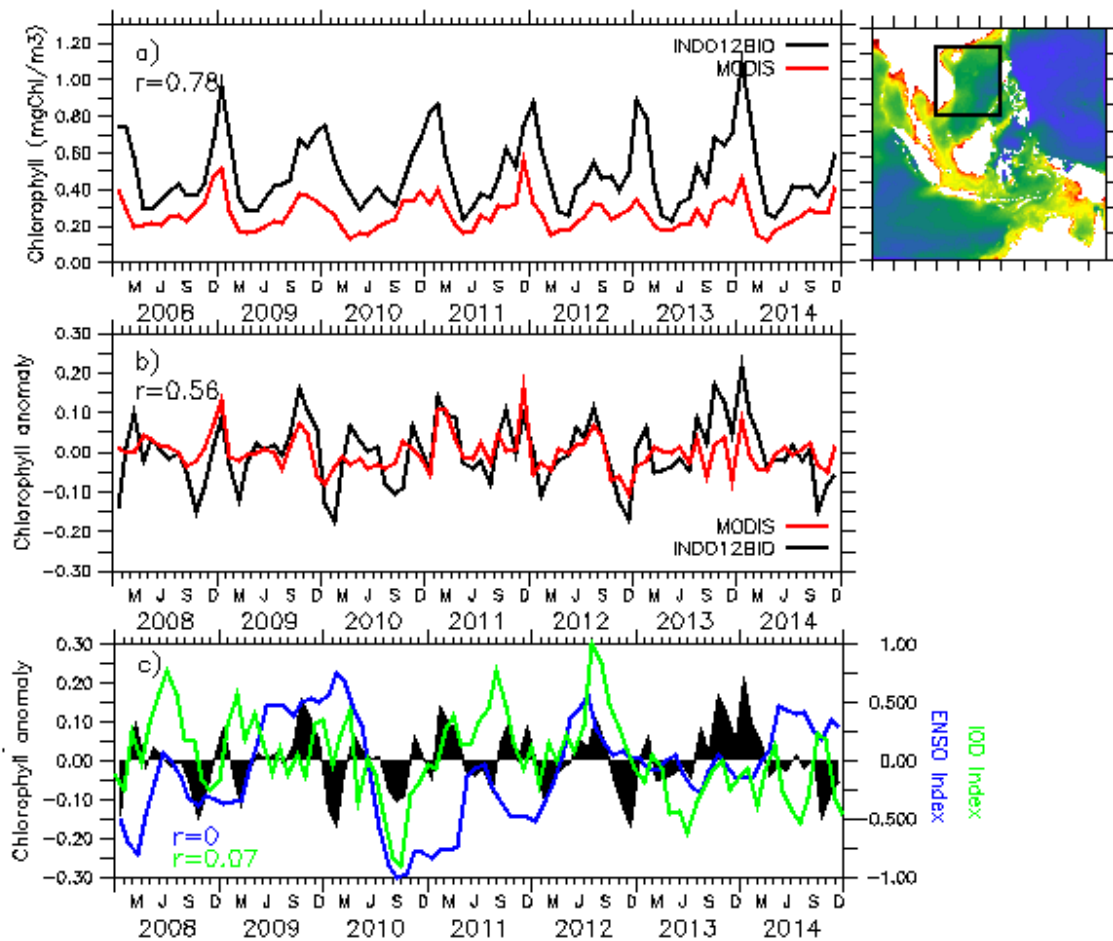


Figure 7: a) Mean surface chlorophyll-*a* concentrations and b) its interannual anomalies (mg Chl m⁻³) over the South China Sea. INDO12BIO is in black and MODIS Case-1 in red. Temporal correlation (r) between both time series is in black. c) ENSO (blue) and IOD (green) phenomena are respectively represented by MEI and DMI indexes. Indexes were normalized by their maximum value in order to be plotted on the same axis. Interannual anomalies of simulated chlorophyll-*a* are reminded in black. Temporal correlation (r) between the simulated chlorophyll-*a* and ENSO (IOD) is indicated in blue (green).

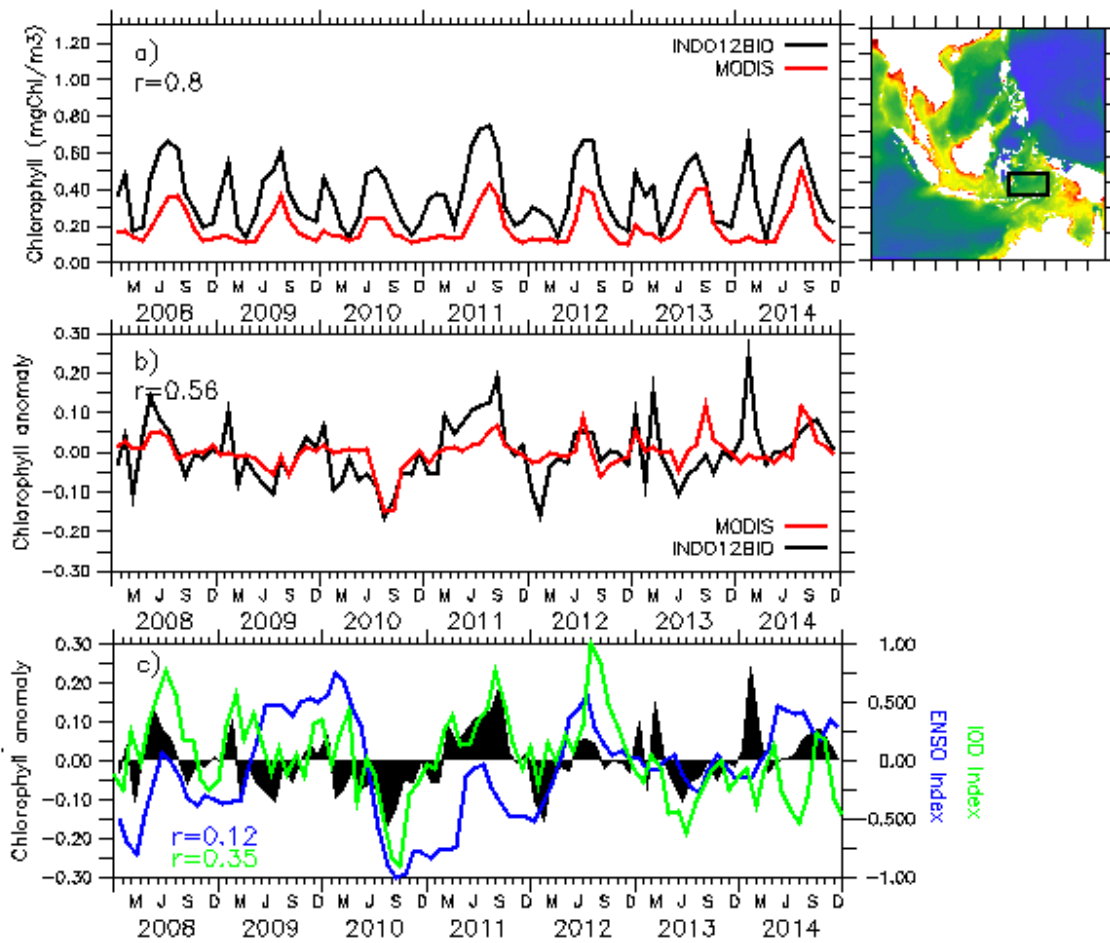


Figure 8: Same as Figure 7, in Banda Sea.

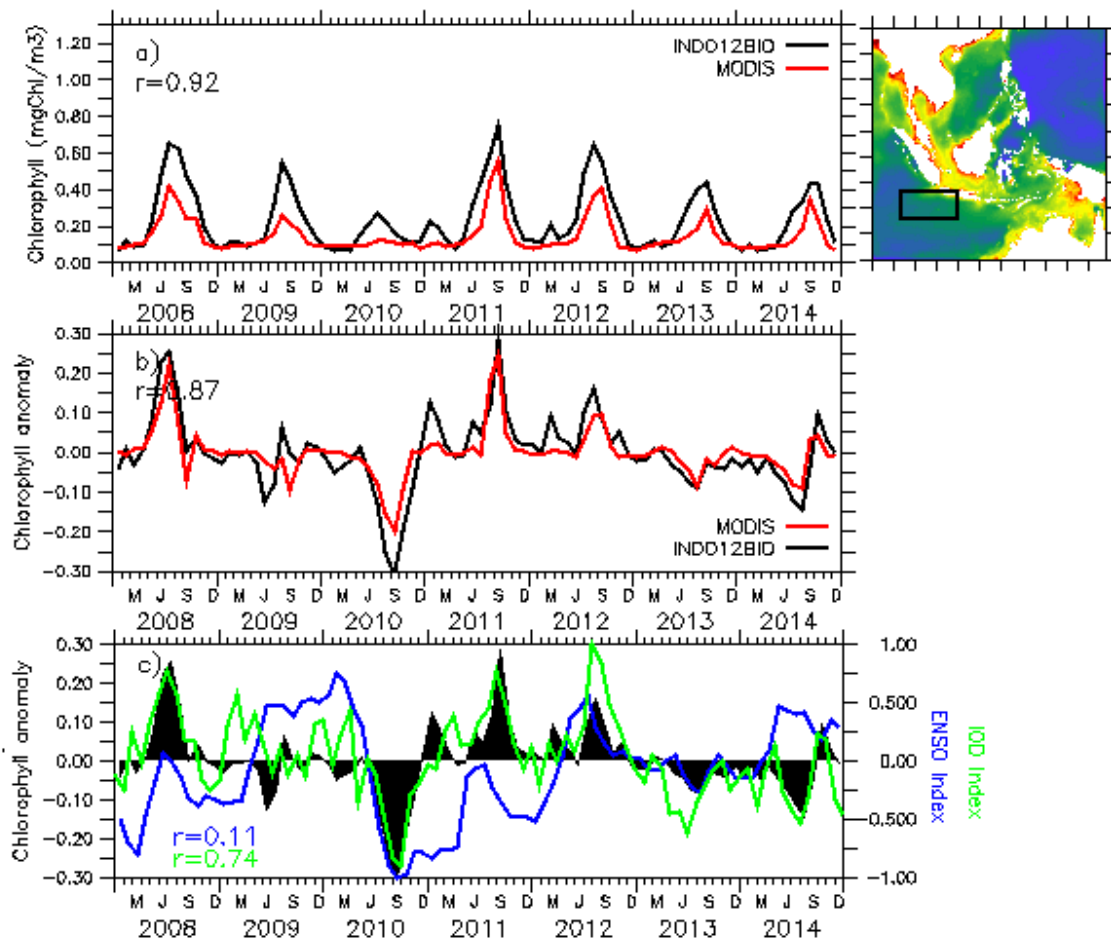


Figure 9: Same as Figure 7, in Sunda area.

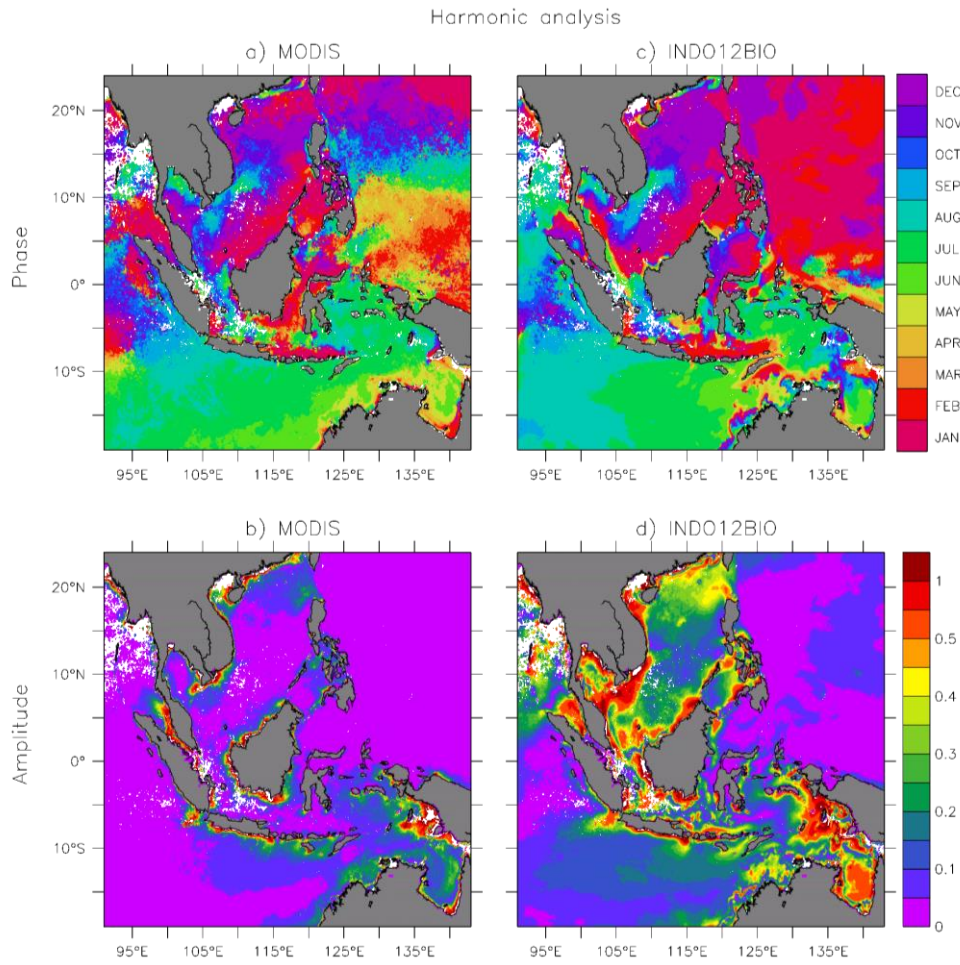


Figure 10. Timing of maximum chlorophyll-*a* (a, c) and amplitude (b, d) for a monthly climatology of surface chlorophyll-*a* concentrations between 2010 and 2014: MODIS Case-1 (left) and INDO12BIO (right). The model was masked as a function of the data.

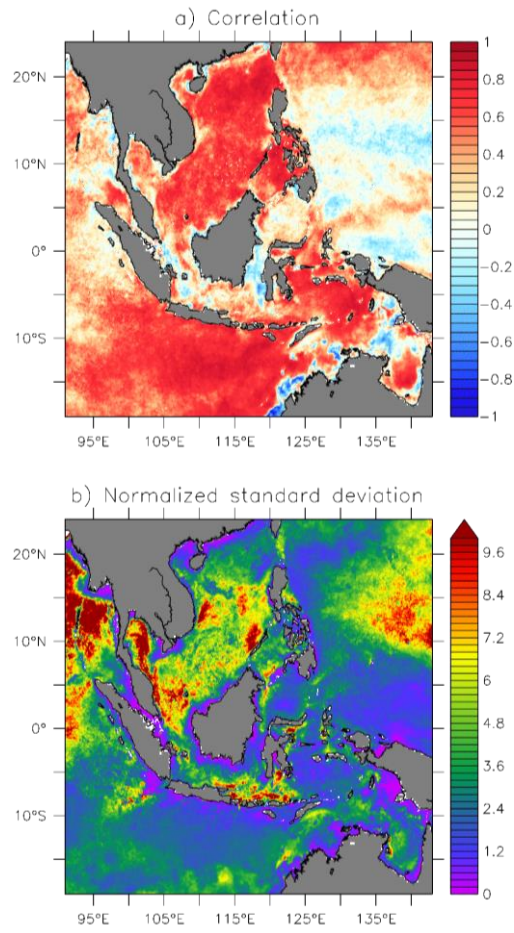


Figure 11: Temporal correlation (a) and normalised standard deviation (b; $\text{std}(\text{model})/\text{std}(\text{data})$) estimated between the INDO12BIO simulation and the MODIS Case-1 ocean colour product. Statistics are computed on monthly fields between 2010 and 2014. The model was masked as a function of the data.

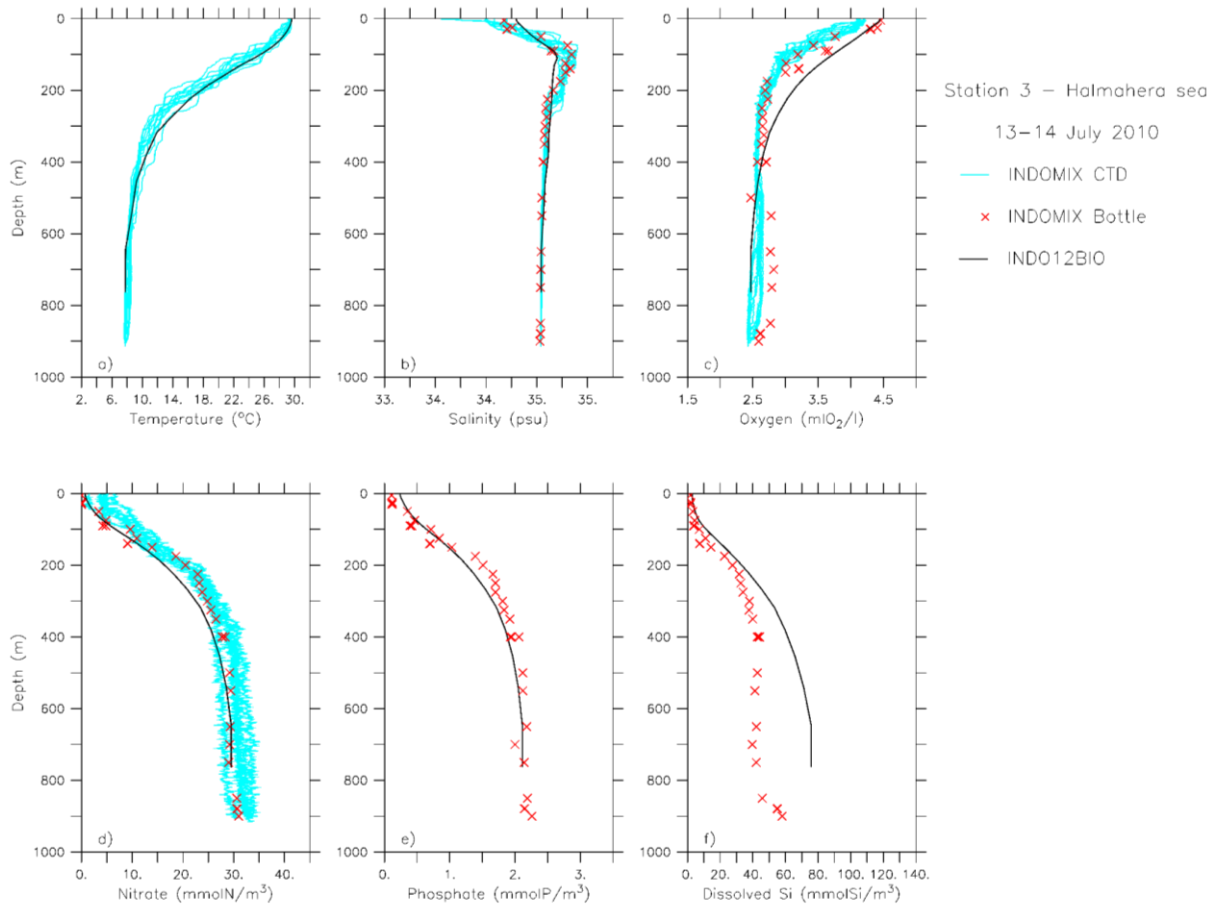


Figure 12: Vertical profiles of temperature ($^{\circ}\text{C}$; a), salinity (psu; b), oxygen ($\text{ml O}_2 \text{ l}^{-1}$; c), nitrate (mmol N m^{-3} ; d), phosphate (mmol P m^{-3} ; e), and dissolved silica (mmol Si m^{-3} ; f) concentrations at INDOMIX cruise Station 3 (Halmahera Sea; 13 - 14 July 2010). CTDO or ISUS sensor (light blue lines) and bottle (red crosses) measurements represent the conditions during cruise, 2-day model averages are shown by the black line.

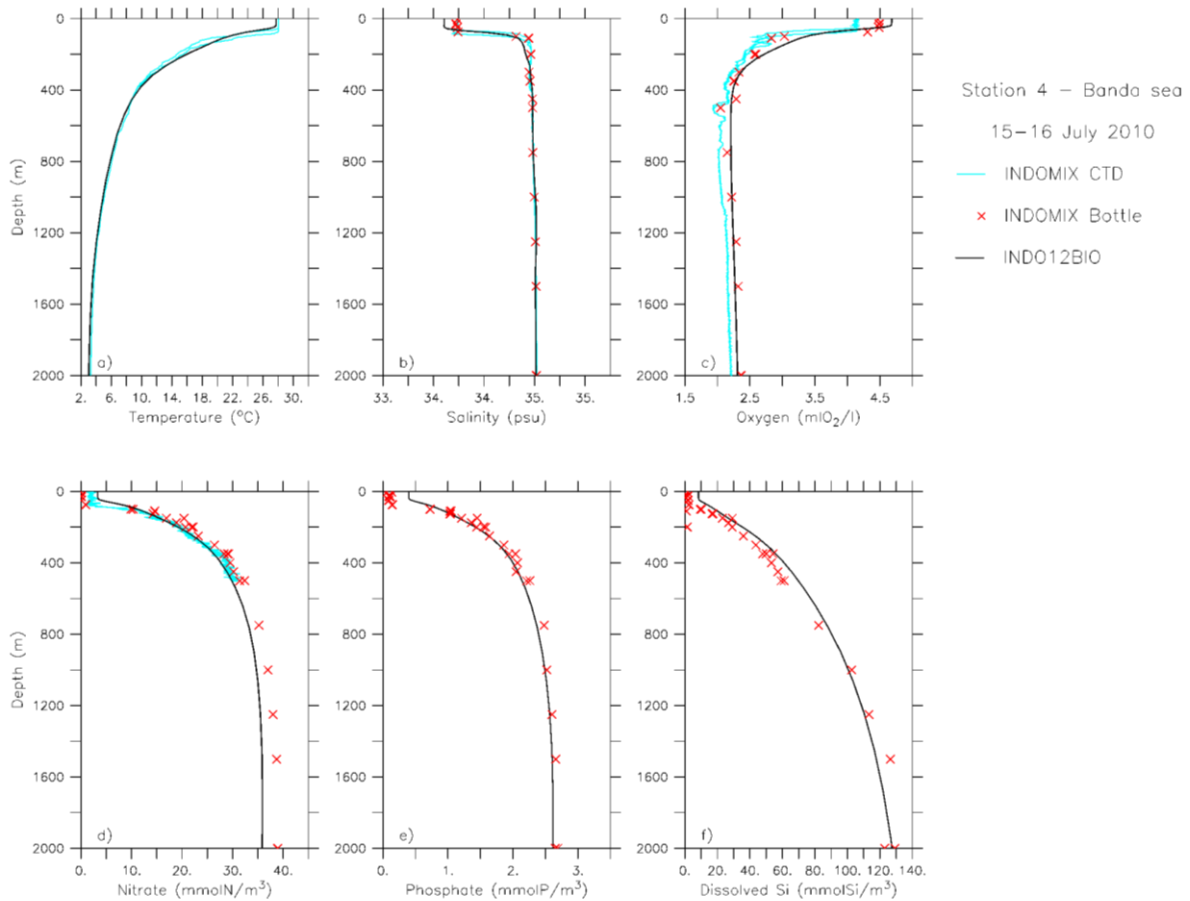


Figure 13: Vertical profiles of temperature ($^{\circ}\text{C}$; a), salinity (psu; b), oxygen ($\text{ml O}_2 \text{ l}^{-1}$; c), nitrate (mmol N m^{-3} ; d), phosphate (mmol P m^{-3} ; e), and dissolved silica (mmol Si m^{-3} ; f) concentrations at INDOMIX cruise Station 4 (Banda Sea; 15 - 16 July 2010). CTDO or ISUS sensor (light blue lines) and bottle (red crosses) measurements represent the conditions during cruise, 2-day model averages are shown by the black line.

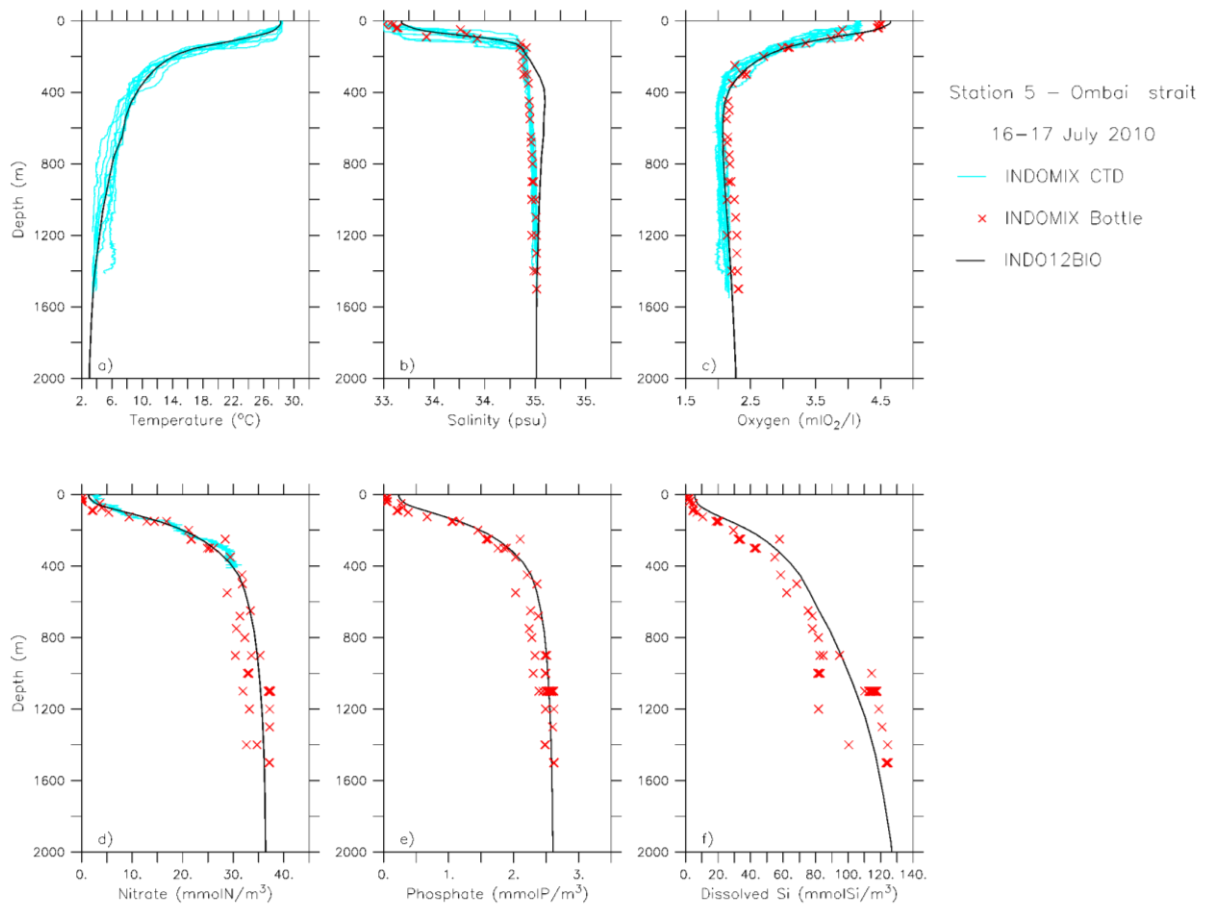


Figure 14: Vertical profiles of temperature (°C; a), salinity (psu; b), oxygen (ml O₂ l⁻¹; c), nitrate (mmol N m⁻³; d), phosphate (mmol P m⁻³; e), and dissolved silica (mmol Si m⁻³; f) concentrations at INDOMIX cruise Station 5 (Ombai Strait; 16 - 17 July 2010). CTDO or ISUS sensor (light blue lines) and bottle (red crosses) measurements represent the conditions during cruise, 2-day model averages are shown by the black line.